Interaction of Synthetic HA2 Influenza Fusion Peptide Analog with Model Membranes

Doncho V. Zhelev,* Natalia Stoicheva,* Peter Scherrer,† and David Needham*

*Department of Mechanical Engineering and Materials Science, Duke University, Durham, North Carolina 27708-0300 and †INEX Pharmaceuticals, Vancouver, British Columbia V6P 6P2, Canada

ABSTRACT The interaction of the synthetic 21 amino acid peptide (AcE4K) with 1-oleoyl-2-[caproyl-7-NBD]-*sn*-glycero-3-phosphocholine membranes is used as a model system for the pH-sensitive binding of fusion peptides to membranes. The sequence of AcE4K (Ac-GLFEAIAGFIENGWEGMIDGK) is based on the sequence of the hemagglutinin HA2 fusion peptide and has similar partitioning into phosphatidylcholine membranes as the viral peptide. pH-dependent partitioning in the membrane, circular dichroism, tryptophan fluorescence, change of membrane area, and membrane strength, are measured to characterize various key aspects of the peptide–membrane interaction. The experimental results show that the partitioning of AcE4K in the membrane is pH dependent. The bound peptide inserts in the membrane, which increases the overall membrane area in a pH-dependent manner, however the depth of insertion of the peptide in the membrane is independent of pH. This result suggests that the binding of the peptide to the membrane is driven by the protonation of its three glutamatic acids and the aspartic acid, which results in an increase of the number of bound molecules as the pH decreases from pH 7 to 4.5. The transition between the bound state and the free state is characterized by the Gibbs energy for peptide binding. This Gibbs energy for pH 5 is equal to −30.2 kJ/mol (−7.2 kcal/mol). Most of the change of the Gibbs energy during the binding of AcE4K is due to the enthalpy of binding −27.3 kJ/mol (−6.5 kcal/mol), while the entropy change is relatively small and is on the order of 6.4 J/mol·K (2.3 cal/mol·K). The energy barrier separating the bound and the free state, is characterized by the Gibbs energy of the transition state for peptide adsorption. This Gibbs energy is equal to 51.3 kJ/mol (12.3 kcal/mol). The insertion of the peptide into the membrane is coupled with work for creation of a vacancy for the peptide in the membrane. This work is calculated from the measured area occupied by a single peptide molecule (220 Å^2) and the membrane elasticity (190 mN/m), and is equal to 15.5 kJ/mol (3.7 kcal/mol). The comparison of the work for creating a vacancy and the Gibbs energy of the transition state shows that the work for creating a vacancy may have significant effect on the rate of peptide insertion and therefore plays an important role in peptide binding. Because the work for creating a vacancy depends on membrane elasticity and the elasticity of the membrane is dependent on membrane composition, this provides a tool for modulating the pH for membrane instability by changing membrane composition. The insertion of the peptide in the membrane does not affect the membrane permeability for water, which shows that the peptide does not perturb substantially the packing of the hydrocarbon region. However, the ability of the membrane to retain solutes in the presence of peptide is compromised, suggesting that the inserted peptide promotes formation of short living pores. The integrity of the membrane is substantially compromised below pH 4.8 (threshold pH), when large pores are formed and the membrane breaks down. The binding of the peptide in the pore region is reversible, and the pore size varies on the experimental conditions, which suggests that the peptide in the pore region does not form oligomers.

INTRODUCTION

Hemagglutinin (HA) plays a critical role in the entry of the influenza virus in host cells (Stegmann and Helenius, 1993). It mediates both the initial attachment of the virus to sialic acid containing receptors on the host membrane (Rogers et al., 1983) and the fusion between the viral membrane and the endosomal membrane (Martin et al., 1981). The fusion site contains at least three hemagglutinin homotrimers (Bentz et al., 1990; Danieli et al., 1996). Each HA protein from the homotrimers has two disulfide-linked subunits HA1 and HA2, which at low pH undergo conformational change and mediate fusion of the viral envelope and the host cell membrane (Bentz et al., 1990; Bullough et al., 1994). One of the subunits (HA1) contains the binding site for sialic acid (Sauter et al., 1989), and the other (HA2) contains a highly conserved apolar sequence of about 20 amino acids at its N terminal (fusion peptide), which facilitates the fusion event (Gething et al., 1986; Harter et al., 1989; Durrer et al., 1996). The fusion of the viral membrane with the cell membrane proceeds in several stages. In the first stage, the conformational change of HA2 exposes the fusion peptide about 100 Å from the viral membrane (Bullough et al., 1994). In the second stage, the exposed fusion peptide inserts in the closest membrane, which may be either the host cell membrane or the viral membrane itself (Weber et al., 1994). The insertion of the fusion peptide in the host membrane provides the necessary link between the viral envelope and the cell membrane. The third stage of the fusion event is the creation and the expansion of the fusion pore, which ultimately results in the mixing of the volume contents of the virus and the cell (Bentz, 2000). Between the second and the third stage there is an intermediate stage,

Received for publication 15 December 2000 and in final form 4 April 2001.

Address reprint requests to Doncho V. Zhelev, Duke University, Dept. Mech. Eng. and Material Science, Durham, NC 27708-0300. Tel.: 919-660-5335; Fax: 919-660-8963; E-mail: dvzh@acpub.duke.edu.

0006-3495/01/07/285/20 $2.00

which is very important for fusion, because it determines the direction of the fusion event. In this stage, the viral membrane and the host cell membrane are linked (Gaudin et al., 1995) and reversible conducting pores are formed (Chernomordic et al., 1998). However, the completion of the fusion event depends on the restricted flow of lipid in the pore region (Chernomordic et al., 1998). The transmembrane domain of HA plays an important role in the regulation of this process. The absence of this domain abolishes fusion but not the hemifusion of the two bilayers (Kemble et al., 1994; Melikyan et al., 1995). The role of the transmembrane domain in fusion is rather physical because its substitution with the transmembrane domain of other viral fusion proteins (Schroth-Diez et al., 1998) recovers the fusion capability of HA. This suggests that the role of the transmembrane domain is probably limited to the creation of a physical barrier for the diffusion of the membrane lipids in the pore region (Bentz, 2000).

It is clear from the above mechanism of viral fusion that the HA fusion peptide plays an essential role in the fusion event. The removal of the peptide from the otherwise intact HA results in abolishment of fusion (Ruigrok et al., 1988). Furthermore, the mutations in this region affect the ability of HA2 to fuse membranes, and the substitution of the glycine at the peptide amino-terminal or its removal abolishes fusion completely (Gething et al., 1986). Several studies have been done to reveal the ability of HA2 fusion peptide mutants to insert into membranes (Lear and DeGrado, 1987; Rafalski et al., 1991; Burger et al., 1991; Longo et al., 1997, 1998), or to initiate content leakage (Stegmann et al., 1985; Shangguan et al., 1996; Alford et al., 1994). The ability of the mutants to insert into membranes has been linked to their ability to form α-helical structures (Gray et al., 1996; Takahashi, 1990), however, the ability to form these structures does not guarantee the acquirement of fusogenic capabilities (Burger et al., 1991). Spectroscopy measurements reveal that the folded peptides resign close to the membrane interface, defined by the plane separating the headgroup region and the hydrocarbon region of the membrane lipids (Macosko et al., 1997; Zhou et al., 2000). Also, these measurements show that the peptides inserted at the membrane interface are oriented almost perpendicular to the normal to the membrane surface (Ishiguro, et al., 1996; Zhou et al., 2000). In the continuing effort to reveal the role of the fusion peptides in membrane fusion and to evaluate their ability to trigger the release of encapsulated drugs in a pH-dependent manner, Bailey et al. (1997) characterized the destabilization of model membranes by a lipopetide derived from the influenza hemagglutinin. The lipopetide Lipo-AcE4K was made of the soluble HA synthetic analog AcE4K studied in this work, and the lipid distearoylglycerol. The peptide was anchored to the lipid by its lysine side chain. Bailey et al. (1997), have shown that the lipopetide is capable of anchoring to the target membranes, promoting lipid mixing, and inducing content leakage in a pH-dependent manner. However, the anchored peptide cannot induce membrane fusion and vesicle-content mixing.

AcE4K studied in this work is similar to the soluble peptide E4 studied by Rafalski et al. (1991), except for the acylation of its N terminus and the presence of lysine at its C terminus. E4 can also induce pH-dependent content leakage, however the soluble peptide cannot induce lipid mixing. The inability of the anchored AcE4K peptide to induce vesicle content mixing is consistent with the inability of the GPI-anchored influenza hemagglutinin to induce content mixing (Melikian et al., 1995). However, the comparison of the blue shift of the tryptophan fluorescence and the formation of α-helical structures upon the binding of the Lipo-AcE4K to the membrane (Bailey et al. 1997) with the same characteristics for the soluble E4 (Rafalski et al., 1991), show that the two peptides behave differently. The blue shift for the soluble peptide correlates very well with the formation of α-helical structures (Rafalski et al. 1991), and both characteristics depend on the solution pH. The blue shift of the Lipo-AcE4K is dependent on pH, but the formation of α-helical structures is not (Bailey et al. 1997). This difference can arise from the anchoring of the peptide to the lipid or can be a result of the different primary structure of AcE4K and E4. To reveal the role of the anchoring of the peptide to the lipid in the insertion of AcE4K we characterize, in this work, the binding of AcE4K to 1-stearoyl-2-oleoyl-*sn*-glycero-3-phosphocholine (SOPC) membranes. We determined important thermodynamic characteristics of this binding, such as the Gibbs energy and the enthalpy of binding and the work for creating a vacancy in the membrane, and we compared the experimentally measured characteristics for AcE4K binding to the similar characteristics for the binding of the distearoylglycerol-anchored AcE4K studied by Bailey et al. (1997).

MATERIALS AND METHODS

Materials

The fusion peptide AcE4K with the sequence,

Ac-GLFEAIAGFIENGWEGMIDGK

was synthesized by INEX (Vancouver, Canada). SOPC, 1-oleoyl-2-[caproyl-7-NBD]-*sn*-glycero-3-phosphocholine (OCPC(NBD-6)), 1-palmitoyl-2-stearoyl(6-7)dibromo-*sn*-glycero-3-phosphocholine (PSPC(6-7)Br), and 1-palmitoyl-2-stearoyl(9-10)dibromo-*sn*-glycero-3-phosphocholine (PSPC(9-10)Br), were purchased from Avanti Polar Lipids, Inc. (Alabaster, AL). L-histidine was from (Sigma, St. Louis, MO).

Solution and Vesicle Preparation

Two types of vesicles were used in the experiments: giant vesicles ($\sim$20-μm diameter), used in the micromanipulation experiments, and 100-nm extruded vesicles, used in the bulk experiments. The solutions used for the different types of experiments were also different. The accuracy of the measurements depended strongly on the ability to find buffers, which

would not affect the measured parameters. For example, the vesicle projection length inside the holding pipet measured in the micromanipulation experiments was very sensitive to the change of the solution composition. The projection length changed when the solution used for vesicle preparation was replaced with the buffer solution used to dissolve the peptide. The vesicles were formed in sucrose solution with low ionic strength, whereas the peptide was dissolved in high ionic strength buffered solutions. The buffered solutions could not be used for vesicle preparation because the formed vesicles were very small in size and could not be used for macromanipulation. Then the goal was to find a buffer solution where the change of the vesicle projection length upon solution replacement was small compared to the change of the projection length due to peptide binding. One solution fulfilling this requirement was the solution made of 10 mM L-histidine (Sigma), 50 mM NaCl and 195 mM glucose, with final osmolarity of 305 mOsm. This solution was used in the micropipette experiments. The pH of the buffer was adjusted by adding HCl to decrease its pH or by adding NaOH to increase its pH. After the addition of HCl or NaOH, the osmolarity of the buffer increased. The osmolarity of the buffer was adjusted back to 305 mOsm by adding water.

In the experiments of measuring the permeability of the membrane for water (Olbrich et al., 2000), a single vesicle was transferred from buffer with osmolarity 305 mOsm into buffer with osmolarity of 345 mOsm. The osmolarity of the second buffer was increased by the addition of 40 mM glucose (235 mM total amount of glucose in the solution). Because the presence of histidine in this buffer affects circular dichroism (CD) measurements, the buffers used in the spectroscopy measurements (CD and fluorescence), were made by mixing different amounts of 0.1 M monobasic sodium phosphate and 0.1 M dibasic sodium phosphate. The same buffers were used in all other bulk experiments, such as the measurement of peptide partitioning, and the titration calorimetry measurements.

The giant vesicles used in the micropipette experiments were made as described elsewhere (Needham and Zhelev, 1996). Briefly, 30 microliters of chloroform solution of 1 mg/ml lipid was spread onto a roughened Teflon disk and the chloroform was evaporated under helium. Last traces of solvent were removed by placing the disk in an evacuated desiccator for 2 h (Needham and Nunn, 1990). The so-formed dried lipid layers were prehydrated with water vapor in a helium carrier gas and then fully hydrated overnight in a sucrose solution at 40°C. The osmolarity of the solution was 300 mOsm. The vesicles were resuspended in the experimental solution described above, which contained histidine, NaCl, and glucose.

The extruded vesicles were made either from SOPC or from PSPC(6-7)Br, or PSPC(9-10)Br, depending on the experiment. Stock lipid solution in chloroform (20 mg/ml lipid in chloroform) was dried on the wall of a glass vial by using a stream of helium. The amount of lipid in the preparations varied depending on the experiment. The dried lipid layers were placed in vacuum for at least 24 h to remove the traces of chloroform. The dried lipid was hydrated in the buffer used in the experiments. Lipid hydration was coupled with freezing and thawing of the suspension three times and vigorous vortexing. Finally, the hydrated lipid was extruded seven times through 100-nm polycarbonate filters (Osmonics, Livermore, CA) and used in the experiments.

Micromanipulation

The experimental chamber for the micromanipulation measurements was 3-mm thick and open at both sides, which allowed access to the interior of the chamber. Experiments were performed at room temperature (23°C) using an inverted Nikon microscope with 30× Hofmann modulation optics. The microscope images were recorded using a COHU (San Diego, CA) CCD camera, which was connected to a multiplexer (Model 401, Vista Electronics, La Messa, CA). The micropipettes were made of 0.75 mm OD capillary glass tubing pulled to a fine point with a vertical pipette puller (Model 730, David Kopf Instr., Tujunga, CA) and cut to the desired diameter with a microforge. The pipettes were connected to a manometer system that allowed the applied pressures to be changed and measured to accuracy of 2 microatmospheres. Micropipette suction pressure was measured with differential transducer (Validyne DP15-24, Nortridge, CA). The measured pressure, together with readings of real time, were multiplexed on the recorded images. The recorded images were used to measure the change of the vesicle projection length inside the holding pipette during peptide adsorption and desorption, and during vesicle manipulation. The measurements were done by using calibrated video calipers (Model 305, Vista Electronics).

The experimental set-up for measuring peptide exchange with the membrane was similar to the one used by Needham and Zhelev (1995) to measure the exchange of lysolipids. The assay consists of a holding pipette and two large pipettes. The holding pipette was used to hold a single vesicle and the large pipettes were used to deliver solutions of different composition to the vesicle surroundings. The holding pipette was incubated for 15 min in solution containing 1 wt% bovine serum albumin (Sigma) and then washed with the buffer used in the chamber. The incubation of the holding pipette with albumin minimized the adhesion of the vesicle to the pipette.

Initially, a single vesicle was chosen and held by the holding pipette. The suction pressure in the holding pipette was set to 200 Pa. This pressure was sufficient to keep the vesicle in the pipette while buffer was blown from one of the large pipettes. The membrane tension induced by the suction pressure was on the order of 0.2 $mN \cdot m^{-1}$, which was much smaller than the critical tension for membrane breakdown on the order of 6 to 9 $mN \cdot m^{-1}$ (Needham and Nunn, 1990). After securing the vesicle with the holding pipette, a buffer similar to the one in the experimental chamber was flowed over the vesicle from one of the large pipettes (reference pipette). This allowed the vesicle to establish a reference projection length in the holding pipette during flow conditions. After a steady state was reached, the reference pipette was replaced by the pipette containing peptide solution. The peptide solution was thereby blown over the vesicle and the change of the projection length in the holding pipette was recorded.

When the vesicle was exposed to peptide solution for extended periods of time, the membrane became saturated with peptide. This saturation was observed by the arrest of the vesicle projection length inside the holding pipette. At this point, the suction pressure of the holding pipette was increased and then decreased several times to measure the change of the vesicle projection length as function of the applied membrane tension. Finally, the suction pressure in the holding pipette was increased until the vesicle broke down. These measurements were used to give insight and to make conclusions about the effect of peptide partitioning on membrane integrity and elastic properties. The maximum tension τ_α sustained by the vesicle membrane (called critical membrane tension), was used as a measure for the strength of the membrane. This tension was calculated from the law of Laplace applied to the spherical portion of the vesicle outside the pipette and the spherical cap inside the pipette (Evans and Skalak, 1980),

$$\Delta P = 2\tau_\alpha\left(\frac{1}{R_{\text{pip}}} - \frac{1}{R_{\text{out}}}\right), \tag{1}$$

where ΔP was the applied suction pressure, R_{pip} was the pipette radius and R_{out} was the radius of the outside spherical portion of the vesicle.

The permeability of the membrane for water was determined by measuring the volume change of a single vesicle when it was transferred from low- to high-osmolarity solution. Initially, one of the large pipettes was used to deliver reference solution. After establishing the initial reference state, the solution with high osmolarity was delivered, and the change of vesicle volume was measured. Both the reference solution and the high osmolarity solution contained the same concentration of peptide and had the same pH. The only difference between the two solutions was their osmolarity. The volume change (dV/dt) of the vesicle after its exposure to the high osmolarity solution was characterized by (Olbrich et al., 2000),

$$\frac{dV}{dt} = -L_p A_m RT(c_1 - c_2), \tag{2}$$

where A_m was the membrane area, R was the gas constant, T was the temperature, $(c_1 - c_2)$ was the solute concentration difference (which determined the osmotic pressure difference), and the coefficient L_p was defined by $P_f v_w/RT$, where v_w was the specific volume of water, and P_f was the permeability coefficient.

The barrier energy for peptide dissociation was found from the measured rate of peptide desorption from giant vesicles at different temperatures. The initial state in these measurements was a vesicle membrane saturated with peptide. A vesicle membrane saturated with peptide was obtained by flowing buffer with 10 μM peptide over a single vesicle, until steady state was reached. Then the vesicle was placed in a flow of peptide-free buffer and the decrease of its projection length in the holding pipette was measured. The dependence of the projection length change on time was a single exponential (see Fig. 8 *A*), which suggested that only the peptide that was previously intercalated in the outside monolayer was desorbed. In this case, the number of peptide molecules N_p, remaining in the outside monolayer was given by (Zhelev, 1996),

$$N_p = N_{ip}\exp\left[-\left(\frac{k_{mb}}{1+\frac{A_m k'_{bm}}{p'}}\right)\cdot t\right], \qquad (3)$$

where N_{ip} was the initial number of intercalated peptide molecules, k_{mb} was the rate of peptide transfer from the membrane to the buffer solution, A_m was the membrane area, k'_{bm} was the rate of peptide transfer from the bulk to the membrane, p' was the apparent mass transfer coefficient for the stagnant layer, and t was the time. For the flow rates used in these experiments, the mass transfer coefficient was large and the measured area changes were not affected by the stagnant layer.

Bulk Measurements

Light scattering

Light scattering experiments were performed to test for peptide aggregation of concentrated peptide solutions at different pH. An N4 analyzer (Coulter, Miami, FL) was used for these measurements. Peptide, 3.5 mg, was dissolved in 1 ml of the buffer solution (pH 7.5). The pH of the sample was lowered by adding HCl to the test cell.

Circular dicroism

CD was used to monitor the change of peptide secondary structure in the absence and the presence of lipid for buffers of different pH. The CD measurements were performed with Aviv 62DS spectropolarimeter. The experiments were performed at 25°C using 1-mm-path-length quartz cuvette. The spectra were obtained from 190 to 260 nm with bandwidth 1 nm and acquisition time 1 s. The scan speed was 20 nm/min, and each spectra was average of 30 scans. Each measurement started by adding 200 μl phosphate buffer with the desired pH in the cuvette. The CD spectra of the peptide-free buffer were measured to obtain baseline spectra. Then 10 μl of 0.22 mM peptide solution was added to the buffer and its CD spectra were measured. Finally, to the buffer-peptide solution was added 10 μl vesicle solution (100 nm extruded vesicles) with lipid concentration of 8 mM, and the CD spectra were measured again. The corrected CD spectra for pure peptide and peptide in presence of lipid were obtained by subtracting the baseline for the peptide free buffer from the corresponding spectra.

Tryptophan fluorescence

The measurement of the blue shift and the quenching of the tryptophan fluorescence were performed using spectrofluorimeter model RF-1501 (Shimadzu, Kyoto, Japan). A 0.25-mm quartz cuvette was used in the measurements. All experiments were performed at 25°C. Extruded vesicles, 100 nm, made of SOPC, PSPC(6-7)Br, PSPC(9-10)Br, and PSPC(11-12)Br were used in the measurement of the quenching of the tryptophan fluorescence. The stability of the lipids during the measurements was critical. This stability was tested using NBD-lipids, for which the distance from the fluorophore to the membrane interface was fixed. The membranes used in the test experiments were made of SOPC:OCPC(NBD-6), OCPC(NBD-6):PSPC(6-7)Br, OCPC(NBD-6):PSPC(9-10)Br, and OCPC(NBD-6):PSPC(11-12)Br. In all membranes, the ratio of the NBD-lipid to the tested lipid was (4.5:100). The data from the test measurements showed that SOPC, PSPC(6-7)Br, and PSPC(9-10)Br were stable after multiple exposure to the excitation light of the fluorimeter, but PSPC(11-12)Br was very unstable. Because of this instability, the data with PSPC(11-12)Br membranes were not reported here.

Titration calorimetry

Titration calorimetry measurements were used to determine the enthalpy of binding and the lipid-to-peptide ratio of binding. The measurements were performed using high-sensitivity titration calorimeter (Microcal, Northampton, MA). Initially the calorimeter chamber was filled with 2.5 ml buffer containing 10 μM peptide. Extruded vesicles (100-nm diameter) made in the same buffer were injected in the chamber in increments of 20 μl (except for the first injection, which was 10 μl). The increment of the lipid concentration due to the vesicle injection was 21 mM lipid. The reference chamber of the calorimeter was filled with water.

Light absorption

The light adsorption of tryptophan was used to determine peptide concentration in solutions free of lipid. The measurements were performed using Model UV-1601 spectrophotometer (Shimadsu). The adsorption spectra of the tryptophan for the window from 240 to 400 nm was used to determine peptide concentration. The concentration was determined using the adsorption at 280 nm, and the adsorption spectra from 320 to 400 nm was used for establishing baseline. Peptide concentration was measured for all stock peptide solutions as well as for some of the filtered solutions from vesicle suspensions, when the light scattering and the adsorption by the leaked lipid (lipid-related adsorption) were either negligible or small relative to the peptide adsorption.

Peptide partitioning into membranes

The partitioning of the peptide in the vesicle membrane was measured using a filtration kit (Micropartition Kit, Amicon Inc., Beverly, MA). For the measurement of the partitioning coefficient, 100-nm extruded vesicles were used and only half of the solution in the samples was passed through the filter. The duration of filtration was between half an hour and one hour depending on the vesicle concentration. The temperature of the experiments was 25°C. Peptide partitioning was measured both for the buffer used in the micropipette experiments and the phosphate buffer used in the bulk experiments. The pH of the buffers was changed from pH 7.5 to pH 4.5. Three types of samples were made for each measurement: peptide without lipid, lipid without peptide, and peptide and lipid. For the measurement of partitioning for a given pH, there was one sample with peptide without lipid and several samples with lipid without peptide and lipid with peptide. The peptide concentration in all samples was 10 μM, while the lipid concentration was varied. The lipid concentration was varied until a sample was found for which the bound peptide was from 30% to 70% of the total peptide added. The filters used in this assay allowed some of the lipid to pass, which affected the adsorption measurements. To eliminate the dependence of the measured adsorption at 280 nm, on the "leaked" lipid, the spectra of the filtered lipid with peptide sample was compared to the spectra of filtered lipid without peptide sample. Several samples were compared until a matching pair of spectra was found. Two spectra were considered a matching pair when the adsorption for the short and the long wavelengths was similar. To improve the ability to compare the spectra, the

adsorption was measured in the range from 210 to 400 nm. The sample with peptide and without lipid was used as a control for the loss of peptide due to peptide binding to the tube wall and to the filter. We found that, for the measured range of pH, the binding of AcE4K to the tube wall and the filter was negligible. These measurements showed that the tubes and the filters from the filtration kit could be used for the measurement of AcE4K partitioning without preincubation with peptide solution.

Peptide binding (reversibility)

The reversibility of peptide binding was confirmed by washing the peptide from a vesicle suspension that initially contained peptide (dilution experiment). For this experiment, vesicles extruded through 200-nm polycarbonate filters were used. The experimental chamber was filled with 2 ml solution containing 5 mg/ml lipid (as extruded vesicles) and 10 μM peptide. The pH of the solution was 5.5, which was the pH of the added solution. Half of the solution from the lipid suspension containing peptide was filtered through a 30-nm filter. The lost volume was recovered by adding 1 ml peptide-free solution to the chamber. The vesicles and the added solution were mixed and another 1 ml solution was filtered. The lost volume was recovered again by adding 1 ml peptide-free solution and so on. The filtered fractions were collected, and the fluorescence intensity of the tryptophan at 350 nm was measured. In a separate experiment, the fluorescent intensity of the tryptophan at 350 nm for peptide solutions with range of concentrations from 0 to 10 μM was measured. The determined dependence of fluorescence intensity on tryptophan concentration was used to determine the amount of peptide in the filtered fractions. The measurement of the fluorescence intensity was the preferred method for determining peptide concentration in this case, because it was very difficult to generate matching samples for the lipid leaked during the filtration.

RESULTS

AcE4K in the membrane and in the solution

We mentioned in the Introduction section that AcE4K was very similar to the peptide E4 studied by Rafalski et al. (1991), except that the N terminal of AcE4K was acylated and it had a lysine at its C terminal. At pH 5, the insertion of E4 in the membrane was coupled with a blue shift of the fluorescence of its tryptophan (Rafalski et al. 1991). Similarly, the fluorescence of the tryptophan of AcE4K was pH dependent, and shifted to short wavelengths as the pH of the solution decreased from pH 8 to 4.5 (Fig. 1). The blue shift of the tryptophan fluorescence indicated that the tryptophan's side chain was transferred from a hydrophilic environment to a more hydrophobic environment (Lakowicz and Keating, 1983). The measurement of the tryptophan fluorescence for peptide solutions in the absence of lipid showed that there was no blue shift (data not shown). This result suggested that there was no measurable peptide aggregation in the 10-μM peptide solution for pH from 8 to 4.5. Similar behavior was observed by measuring the light scattering of concentrated (1.4 mM) peptide solutions in the absence of lipid (data not shown). The light scattering data showed that there was no aggregation of peptide for pH above 4.6. However, for pH below 4.6, there was significant self-aggregation and precipitation of the peptide from the solution. These data showed that there was a threshold pH on the order of 4.5 (depending on peptide concentration), above which the peptide in the solution did not form aggregates. The peptide precipitated from the solution only in the presence of lipid membranes when the pH was below 6. In these conditions, the peptide adsorbed to the lipid membranes, which was documented by the presence of the blue shift.

The observation of the primary structure of AcE4K suggested that it could form α-helical structure and behave as amphiphilic peptide. The measurement of the circular di-

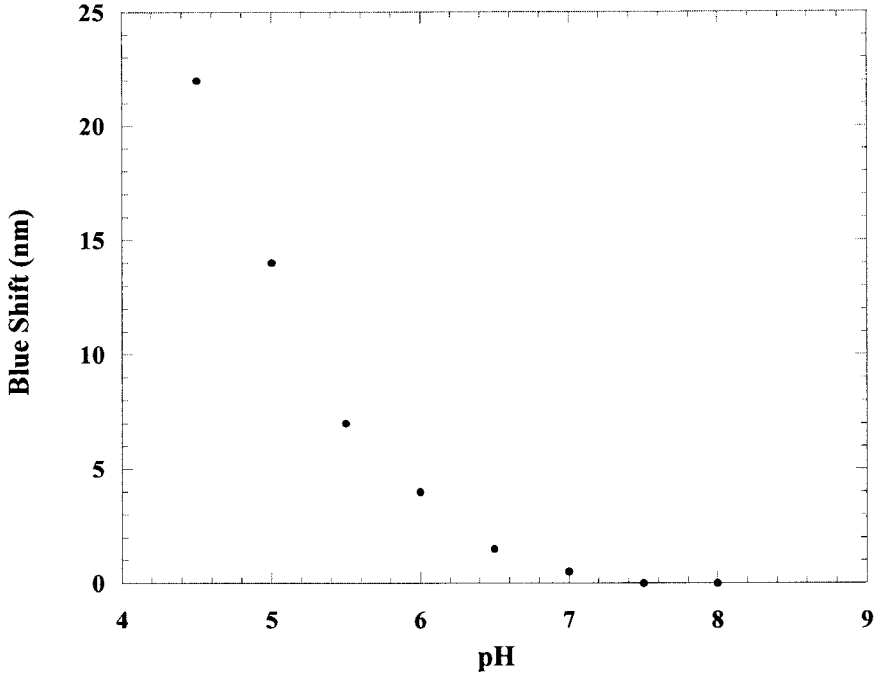

FIGURE 1 Blue shift of the tryptophan fluorescence verses the change of the buffer pH. The peptide concentration was 10 μM, and the lipid concentration was 0.38 mM.

chroism spectra of the Lipo-AcE4K by Bailey et al. (1997) showed that, indeed, the lipid-anchored AcE4K formed α-helical structures. However, the measured α-helical structures for the Lipo-AcE4K were independent of pH (Bailey et al. 1997), and the tryptophan fluorescence had a blue shift (Bailey et al. 1997). It was not clear from the measurements of Bailey et al. (1997) whether the pH-independent α-helical structures of the Lipo-AcE4K were a result of the interaction of the anchored peptide with the membrane to which the peptide was anchored, or it was a property of the peptide itself. For each pH, we measured the CD spectra for AcE4K in the absence and the presence of lipid (see Materials and Methods). These measurements showed that, in the absence of lipid, AcE4K was in random coil conformation regardless of the solution's pH. In the presence of lipid membranes, the measured CD spectra showed pH-dependent formation of α-helical structures (Fig. 2 *A*). These measurements showed also that there were only two distinct secondary structures: random coil (possibly from the peptide in the solutions) and α-helical (possibly from the peptide bound to the membrane) (Fig. 2 *A*). The transition from one conformation to the other occurred as the pH changed from 8 to 4.5. For pH 4.5, the helicity of the peptide was close to the 100% theoretical helicity calculated from the model used by Chang et al. (1978). Then the helicity measured for pH 4.5 was considered a good estimate for the maximum helicity of AcE4K. The change of helicity was characterized by the change of the measured ellipticity at 222 nm (Fig. 2 *B*). The comparison of Fig. 2 *B* and Fig. 1 showed that the change of peptide helicity correlated very well with the tryptophan blue shift. Therefore, both the blue shift and the increase of peptide helicity indicated that AcE4K had a tendency to bind to the membrane when the pH decreased from 6 to 4.5.

The folded AcE4K was expected to be amphiphilic and most likely partitioned at the membrane interface. The observation of the helical wheel of AcE4K (not shown) suggested that the side chain of the triptophan should be close to the membrane interface. The anticipated position of AcE4K in the membrane was similar to the position of the wild-type HA2 fusion peptide. The wild-type peptide resigned at the membrane interface and was almost perpendicular to the normal of the membrane surface (Zhou et al., 2000). To confirm this assumption, we measured the depth of insertion of the tryptophan side chain in the membrane and compared it with the depth of insertion of the tryptophan of the wild-type HA2. We used the paralax method developed by Chattopadhyay and London (1987) for the measurement of the depth of insertion of the tryptophan side chain.

The paralax method used the quenching of the tryptophan's fluorescence by dibromo lipids. The method required almost all of the peptide molecules to be bound to the membrane. The binding of the peptide was monitored by measuring the blue shift of preparations containing the same amount of peptide (10 μM), and increasing the amount of lipid. The maximum blue shift for solution with pH 5, was measured for lipid concentrations on the order of 3 mM (not shown). To ensure maximum binding, the measurements of tryptophan quenching were performed using samples containing 10 μM peptide and 5.5 mM lipid. The maximum quenching was measured for the membranes made of PSPC(6-7)Br, and the minimum quenching was measured for the pure SOPC membranes (no bromo-substitution were present) (Fig. 3). The maximum quenching for the membrane made of PSPC(6-7)Br suggested that the tryptophan side chain was closer to the sixth and the seventh carbon in the lipid acyl chain than to the ninth and the tenth carbon. The distance z_{F1} of the tryptophan from the shallower quencher (PSPC(6-7)Br) was determined by (Chattopadhyay and London, 1987)

$$z_{F1} = \pm\left(\frac{L_{12}^2 + (1/\pi C)\ln(F_1/F_2)}{2L_{12}}\right), \qquad (4)$$

where L_{12} was the distance between the two quenchers, C was the quencher concentration per unit membrane area (in this case, the area occupied by the two quenchers was equal to the area of one lipid molecule), the ratio F_1/F_2 was the ratio of the intensity of the tryptophan fluorescence from the membrane containing the shallower quencher to the tryptophan fluorescence from the membrane containing the deeper quencher. The distance z_{F1} was positive when the tryptophan was between the two quenchers and negative when the tryptophan was closer to the membrane interface than to the shallower quencher.

The distance between the shallower quencher and the tryptophan was calculated using the following parameters. The area of one PC molecule was assumed equal to 65 Å^2 (McIntosh and Simon, 1986). This corresponded to quencher concentration on the order of 0.031 (1/Å). The ratio F_1/F_2 was 0.28, and the distance between the quenchers was 3.75 Å. Then the calculated distance z_{F1} was 0.1 Å. Therefore, the tryptophan side chain was almost at the same depth as the shallower quencher. The distance of the shallower quencher to the membrane interface (which was considered to be close to the carbonyl groups), was on the order of 8 Å. Then the tryptophan side chain was 8 Å from the membrane interface. This was in good agreement with the distance from the tryptophan back-bone to the lipid phosphate group on the order of 5 Å measured with EPR (Zhou et al., 2000), which placed the tryptophan side chain 5 Å from the membrane interface.

Tryptophan quenching was also measured for pH 6 using the same procedure as the one already described for pH 5. The ratio F_1/F_2 for the solution with pH 6, was equal to 0.28, which was equal to the same ratio for pH 5. This result showed that the depth of insertion of AcE4K in the membrane was independent of pH. This observation was in agreement with the data of Luneberg et al. (1995) and Zhou

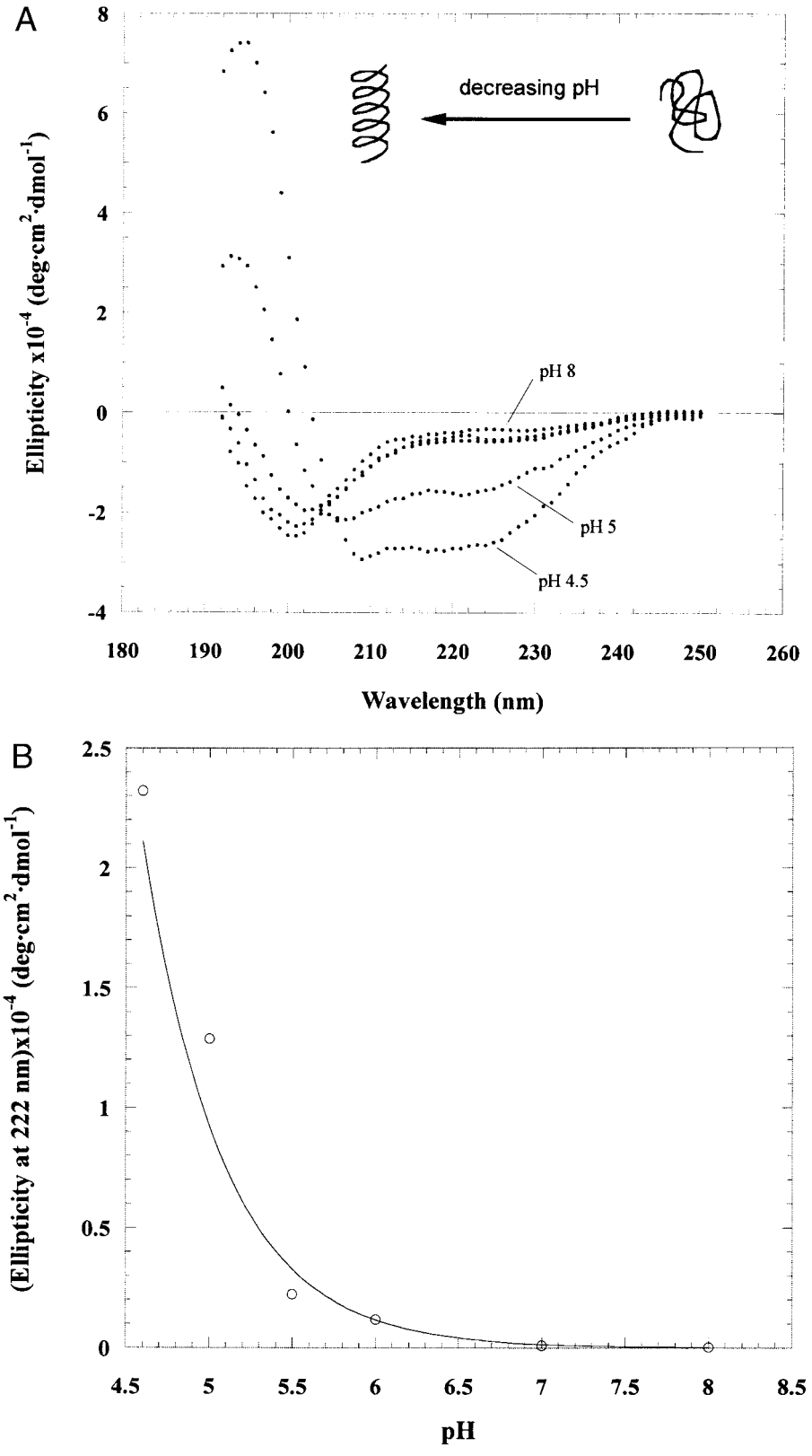

FIGURE 2 (*A*) CD spectra for AcE4K for lipid containing solutions with different pH. The peptide concentration was 10 μM, and the lipid concentration was 0.36 mM. The solid curve represents the calculated spectra for 100% ellipticity (see text). In the absence of lipid, the peptide remained in random coil conformation for the range of pH studied. In this case, the measured CD spectra (not shown) were almost identical to the CD spectra measured for lipid containing solutions at pH 8. (*B*) Change of AcE4K ellipticity at 222 nm verses pH.

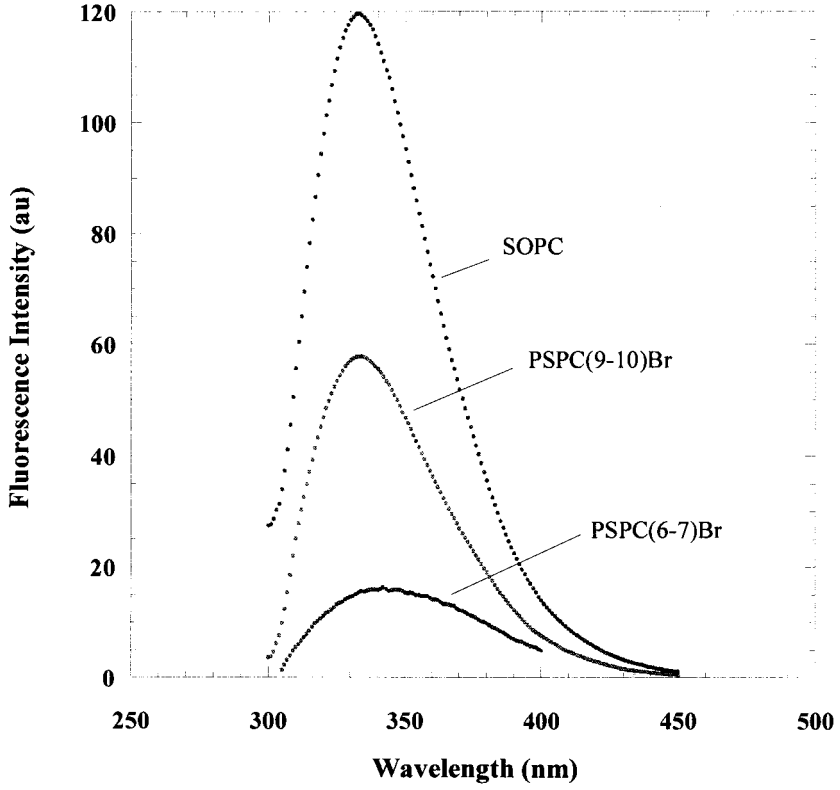

FIGURE 3 Fluorescence intensity of tryptophan from AcE4K inserted in SOPC membranes and membranes made of di-bromo lipids. The peptide concentration was 10 μM, and the pH was 5.

et al., (2000), who also showed that the depth of insertion of the wild-type HA2 fusion peptide was independent of pH.

Thermodynamics of AcE4K binding

The data presented so far suggested that the binding of AcE4K to the membrane was coupled with a conformational change from random coil to α-helical and with the insertion of the folded peptide at the membrane interface. The transfer of the peptide from the solution to the membrane interface depended on several energy characteristics, such as the change of the Gibbs energy, the change of the enthalpy and the entropy of the peptide–membrane complex, and the barrier energy for peptide transfer to and from the membrane. We used a simple thermodynamic model for characterizing peptide binding, where the bound state and the free (unbound) state of the peptide were separated by a single energy barrier.

The measurement of peptide partitioning (Fig. 4 *A*) with the filtration method (see Materials and Methods) showed that the amount of bound peptide increased relative to the free peptide, when the pH of the solution decreased from pH 7.5 to 4.5. We assumed that, for pH below 5.5, all peptide in the solution was available for binding. Then, for any given amount of lipid, the ratio of the concentration of the free peptide to the initial peptide concentration (total peptide), depended on the partition coefficient and the lipid concentration. The ratio of the free peptide to the total peptide was

$$\frac{\text{free peptide}}{\text{total peptide}} = \frac{1}{1 + K_p[L]}, \tag{5}$$

where $[L]$ was the amount of lipid (mol) divided by 55.56, which accounted for the cratic contribution to the binding equilibrium, and K_p was the partition coefficient.

The binding of the peptide to the membrane could also be viewed as a two-step process, where the peptide molecules were initially protonated and then the protonated species could bind to the membrane. In this scenario, not all peptide molecules would be available for binding, and the ratio of the free peptide to the total peptide would deviate from the dependence predicted by Eq. 5. When the protonation is coupled with the binding of the peptide to the membrane, Eq. 5 would hold. (The coupling between the binding of the peptide to the membrane and its protonation is sometime referred to as an apparent increase of the pH for protonation in the presence of membranes.) The data in Fig. 4 *B* showed that the measured ratio of the free peptide to the total peptide was represented adequately by Eq. 5. The good agreement between the experimental data and the curve calculated from Eq. 5 suggested that all peptide molecules in the solution were available for binding. In this case, the partition coefficient K_p was equal to the equilibrium con-

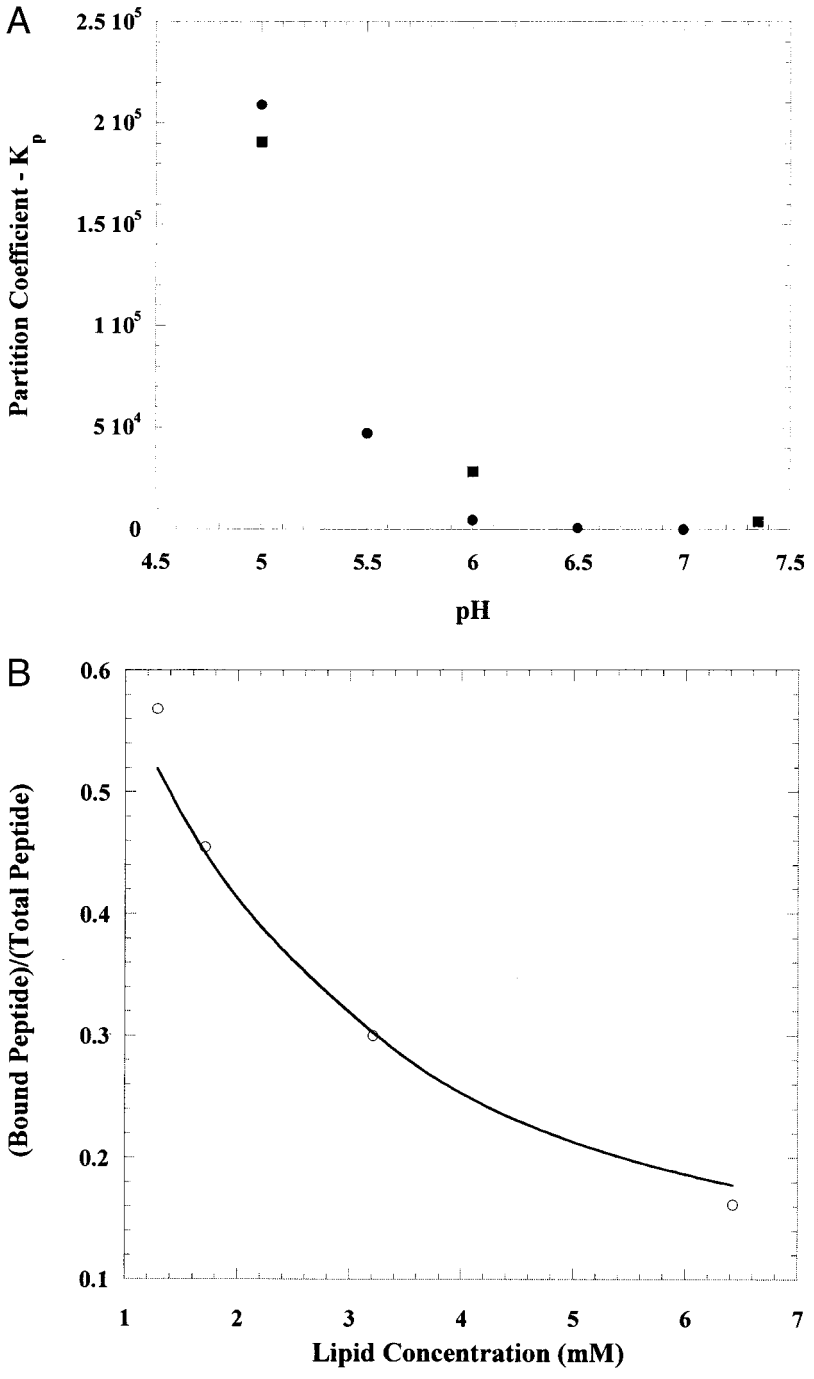

FIGURE 4 (*A*) Partition coefficient for SOPC membranes determined with the filtration method. The circles represent the data points for vesicles in phosphate buffer, and the squares are the data points for vesicles in the buffer used in the micropipette experiments (see Materials and Methods). The partition coefficient for pH 4.5, which is not shown in the graph, was 1×10^6. (*B*) Ratio of the bound peptide to the total peptide verses the lipid concentration, and the prediction of the model, assuming that all peptide in the solution was available for binding. The peptide concentration was 10 μM, and the pH was 5.5.

stant K. Therefore, we used the measured partition coefficients for the calculation of the Gibbs energy ΔG^0 for peptide transfer from the solution to the membrane,

$$\Delta G^0 = -RT \ln K_p, \tag{6}$$

where R was the gas constant and T was the temperature.

The measured partition coefficient for pH 5.5 (Fig. 4 *A*) was on the order of 4.8×10^4. The standard Gibbs energy corresponding to this partition coefficient was -26.7 kJ/mol (-6.4 kcal/mol). The partition coefficient for pH 5 was on the order of 2×10^5, and the corresponding Gibbs energy was -30.2 kJ/mol (-7.2 kcal/mol). The partition coefficients and the corresponding Gibbs energies could also be calculated from the blue shift data in Fig. 1, and the ellipticity data for 222 nm from Fig. 2. The CD spectra in Fig. 2 showed that the helicity for pH 4.5 was almost 100%, thus suggesting that almost all peptide was bound to the membrane. The solution contained 0.36 mM lipid and at pH 8, almost all peptide was free. Then the ratio of the bound verses free peptide for pH 5, calculated from the measured

ellipticities at pH 4.5, 5, and 8, was on the order of 1.3. The partition coefficient corresponding to this ratio was 2×10^5. Similarly, the lipid concentration in the blue shift experiments (Fig. 1), was 0.38 mM, and the ratio of the bound to the free peptide at pH 5 was 1.4. The partition coefficient corresponding to this ratio was 2×10^5. The partition coefficients determined from the three types of measurement, filtration, CD, and tryptophan fluorescence, were very similar. This similarity suggested that both the measured blue shift and the measured change of peptide helicity were directly related to the increased amount of bound AcE4K to the membrane when the pH decreased.

The enthalpy of binding of AcE4K to the SOPC membranes was measured using titration calorimetry. In these experiments, concentrated lipid solution (42 mM maximum concentration), as 100-nm extruded vesicles, was injected into a solution containing 10 μM peptide (Seelig, 1997). After the injection, the vesicles started to mix with the solution in the chamber, and the peptide started to bind to the vesicle membranes. The heat transfer during this process was measured. Similar measurements were performed for the injection of lipid vesicles in a chamber containing peptide-free buffer. The difference between the measured heat transfer in the two cases was used to determine the enthalpy of peptide binding (Fig. 5). The fitting of the experimental data showed that the enthalpy of AcE4K binding was on the order of $\Delta H^0 = -27.3$ kJ/mol (-6.5 kcal/mol), and the lipid-to-peptide ratio was 180 lipids per peptide. The binding constant was not determined from the titration calorimetry data because of uncertainties in their interpretation (Seelig, 1997). The titration calorimetry measurements were performed at pH 5. The comparison of the Gibbs energy for pH 5 and the enthalpy of binding allowed the calculation of the entropy change ΔS^0 during binding. The entropy change was determined from $\Delta G^0 = \Delta H^0 - T\Delta S^0$, and was equal to $\Delta S^0 = 6.4$ J/mol.K (2.3 cal/mol.K). Finally, the heat released during peptide binding was positive, suggesting that AcE4K binding was exothermic.

Exchange of ACE4K with SOPC membranes

The data presented so far provided equilibrium characteristics for the binding of AcE4K to the membrane. We used the micropipette assay developed in our laboratory (Needahm and Zhelev, 1995) to study the kinetics of exchange of the peptide with the membrane. In this assay, a single vesicle was held by a pipette and solutions of different composition were delivered in the surroundings of the vesicle using two large micropipettes. After the exposure of the vesicle to 10 μM AcE4K solution at pH 5.5, the vesicle projection length inside the holding pipette increased. This increase of the vesicle projection length could be either a result of the increase of the vesicle area due to the insertion of the peptide molecules in the membrane, or the decrease of the vesicle volume due to the formation of pores and loss of solute. The contribution of the change of the vesicle area to the change of the projection length was determined from the comparison of the data from two series of measurements. In the first series, a single vesicle was exposed to peptide solution for 21 min (1260 s) by flowing peptide solution from a large pipette (Fig. 6, *open circles*). The peptide from

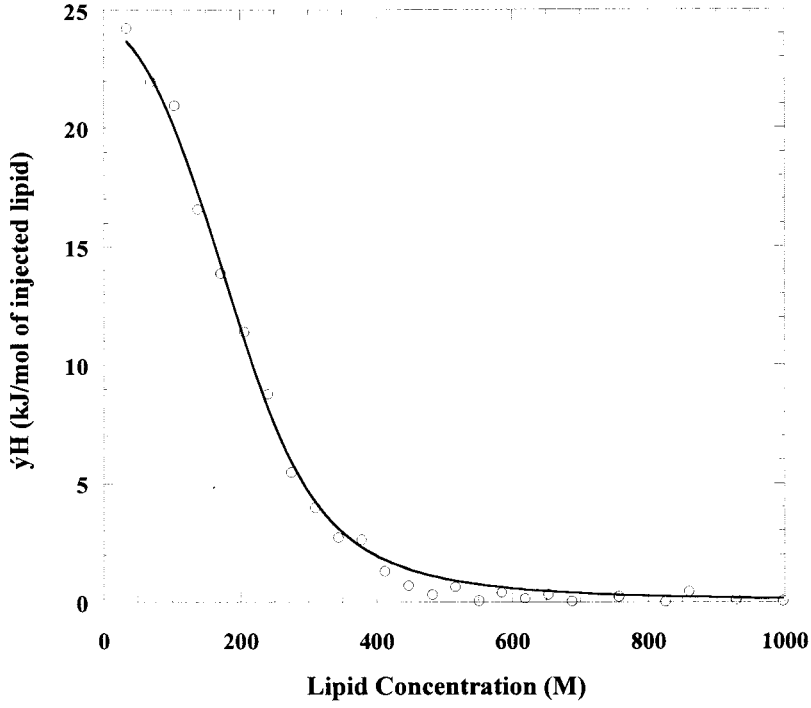

FIGURE 5 AcE4K binding measured with titration calorimetry. The peptide concentration was 10 μM, the pH was 5, and the temperature was 25°C. 100-nm extruded vesicles were injected in the peptide solution.

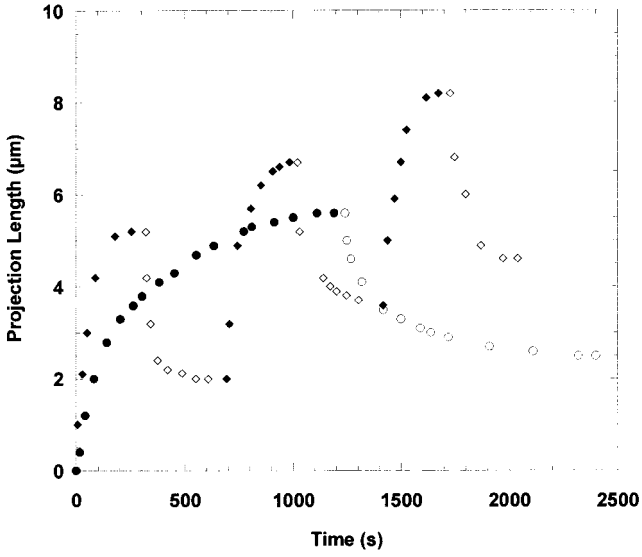

FIGURE 6 Peptide adsorption and desorbtion at pH 5.4. A single vesicle was exposed continuously to peptide buffer for 21 min (*closed circles*) and then the peptide was washed (*open circles*) with peptide-free buffer at the same pH. Another vesicle of similar size was exposed to peptide buffer (*closed diamonds*) and then washed (*open diamonds*) three times with peptide-free buffer. The total time of exposure of the two vesicles to peptide solution was the same. The projection length change after every washing of the adsorbed peptide was similar, and the final residual increase of the vesicle projection length was similar for the two vesicles. The change of the projection length during peptide desorption corresponded to 6% change of the vesicle area.

the solution was adsorbed to the vesicle membrane and the projection length in the holding pipette increased. Then the vesicle was exposed to peptide-free solution and the peptide desorbed, which was coupled with a decrease of the vesicle projection length (Fig. 6). In the second series of measurements, a single vesicle was exposed to peptide solution for 7 min (420 s) and then the peptide was desorbed using the same assay as in the first series. The exposure of the vesicle to peptide solution and the peptide desorption were repeated two times, which provided the same total time of exposure to the peptide solution (21 min), as in the first series. The vesicles used in these measurements had similar sizes and the used holding pipettes had similar radii, which provided similar changes of the vesicle projection length for similar area and volume changes. The comparison of the data from the two series of measurements (Fig. 6), showed that the increase of the vesicle projection length during peptide adsorption was larger for longer exposure to peptide solution. In contrast, the change of the projection length during peptide desorption was similar in all cases. These data could be explained either by assuming that only part of the adsorbed peptide could be desorbed (partial desorption), or that the insertion of the peptide in the vesicle membrane induced content leakage and therefore volume change. In this case, the change of the projection length during peptide desorption was coupled with the change of membrane area due to the decrease of the membrane area occupied by the inserted peptide.

Partial desorption would take place only when two peptide species were present, one with low affinity of binding to the membrane and another with high affinity of binding. The mass spectrometry and HPLC measurements showed that there was only one species in the peptide samples. Nevertheless, we tested the possibility of the presence of nondesorbing species by performing the dilution experiment described in the Materials and Methods section (Fig. 7). From the data of this experiment, it was clear that the total amount of washed peptide (after correcting for the dilution of the peptide in the filtered fractions), was almost equal to the amount of peptide added to the experimental chamber. (The initial peptide concentration was 10 μM, and the apparent concentration of the washed peptide calculated from the concentrations of the fractions in Fig. 7 was 12 μM.) The similarity of the amount of washed peptide and the initial amount of the added peptide, showed that almost all peptide was desorbed. Therefore, the residual increase of the vesicle projection length in the micropipette after AcE4K desorption (Fig. 6) was a result of vesicle volume change. The comparison of the data from the two sets of measurements in Fig. 6 showed also that the residual increase of the vesicle projection length was almost linearly dependent on the time of incubation with the peptide solution. It seems then, that the presence of peptide inserted in the vesicle membrane did, in fact, induce leakage of vesicle content resulting in a decrease of the vesicle volume (the vesicle was held under low but significant suction pressure and so any reduction in the permeability of the membrane to the encapsulated solute could cause vesicle deflation).

During peptide desorption, the highest amount of peptide was present in the membrane in the initial state, just before transferring the vesicle to peptide-free solution. As the peptide started to desorb, its amount in the membrane decreased. Therefore, during peptide desorption, the overall exposure of the membrane to the inserted peptide was relatively small compared to the membrane exposure during peptide adsorption. Also, the time of desorption was very short, on the order of 5–15 s (Fig. 8 *A*), whereas the time for reaching a steady state during peptide adsorption was longer than 5 min. Thus, the measured change of the vesicle projection length during peptide desorption was considered to represent the change of the vesicle area only. The measured relative change of the vesicle area during peptide desorption at pH 5.5 was on the order of 6%.

Another characteristic of the binding of AcE4K to the membrane was the energy barrier, which separated the bound state and the unbound state of the peptide. This barrier was characterized by the Gibbs energies of the transition state. There were two Gibbs energies of transition state, one for the transition from free state to the transition state (Gibbs energy of adsorption ΔG_a^{++}), and another for

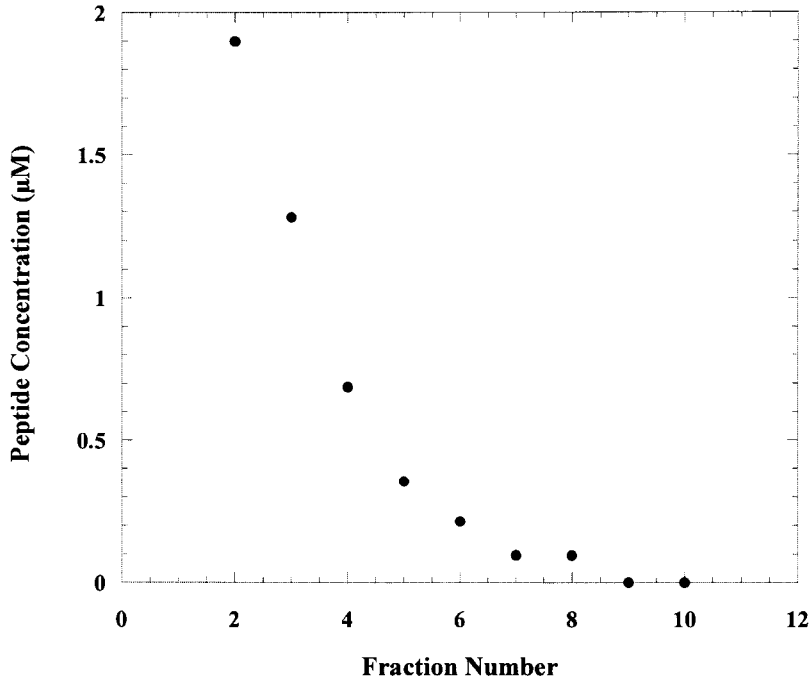

FIGURE 7 Peptide concentration of the sample fractions in the dilution experiment. The dilution for each fraction was 1:1. The peptide concentration in every following fraction was half of the concentration in the previous fraction. The initial peptide concentration in the sample was 10 μM, and the pH was 5.

the transition from bound state to the transition state (Gibbs energy of desorption ΔG_d^{++}). The difference of the two transition Gibbs energies was equal to the Gibbs energy ΔG^0 for peptide transfer from the solution to the membrane. The Gibbs energy of AcE4K desorption was calculated from the measured rate of peptide desorption for different temperatures (Fig. 8 *A*) and the corresponding barrier energy of desorption E_d. The rate of peptide desorption k_- and the barrier energy E_d were related by the Arrhenius equation,

$$\ln k_- = \ln X - \frac{E_d}{RT}, \tag{7}$$

where X was a constant independent of temperature. The barrier energy was found from the slope of the dependence of the rate of peptide desorption on the reciprocal of the temperature. The Gibbs energy of the transition state ΔG_d^{++} was calculated from the barrier energy using

$$\Delta G_d^{++} = \Delta H_d^{++} - T\Delta S_d^{++},$$

$$\Delta H_d^{++} = E_d - RT,$$

$$\Delta S_d^{++} = R\left(\ln\left(\frac{X_0 h N_A}{RT}\right) - 1\right), \tag{8}$$

where ΔH_d^{++} and ΔS_d^{++} were the enthalpy and the entropy of the transition state, T was the temperature, E_d was the barrier energy for desorption, R was the gas constant, X_0 was the intercept from the Arrhenius plot in Fig. 8 *B*, h was the Plank's constant, and N_A was the Avogadro's number.

The data in Fig. 8 *A*, showed that the measured kinetics of the change of the relative projection length (which was related to the relative area change), during peptide desorption was a single exponential. The rate of desorption was chosen equal to the exponential factor of this dependence. The dependence of the rate of peptide desorption on the reciprocal of the temperature shown in Fig. 8 *B*, allowed to determine the barrier energy for desorption. This energy was equal to -47.5 kJ/mol (-11.3 kcal/mol). The coefficient X was determined from the intercept in Fig. 8 *B*, and was 5×10^{-10} (1/s). Then the Gibbs energy of peptide desorption was 78.5 kJ/mol (18.8 kcal/mol).

The measurement of the partitioning of AcE4K in the SOPC membrane showed that the partitioning of the peptide was pH dependent. Therefore, if peptide partitioning was coupled with actual peptide insertion, we expected to observe larger area changes for the same bulk concentration of the peptide when the pH of the solution was decreased from pH 7 to 4.5. Indeed, the data in Fig. 9 showed that the steady-state projection lengths increased with the decrease of the solution's pH. The increase of the projection length with the decrease of the pH provided a direct indication that the adsorbed peptide was inserted in the membrane. In these measurements, the vesicles were stable for solutions having pH above 4.8 (in these conditions, the vesicles remained stable for more than half an hour). However, for pH below 4.8, the vesicles were very unstable and broke during the initial adsorption of the peptide (Fig. 9). This behavior was different from the equilibrium bulk measurements, where the measured characteristics (peptide partitioning, trypto-

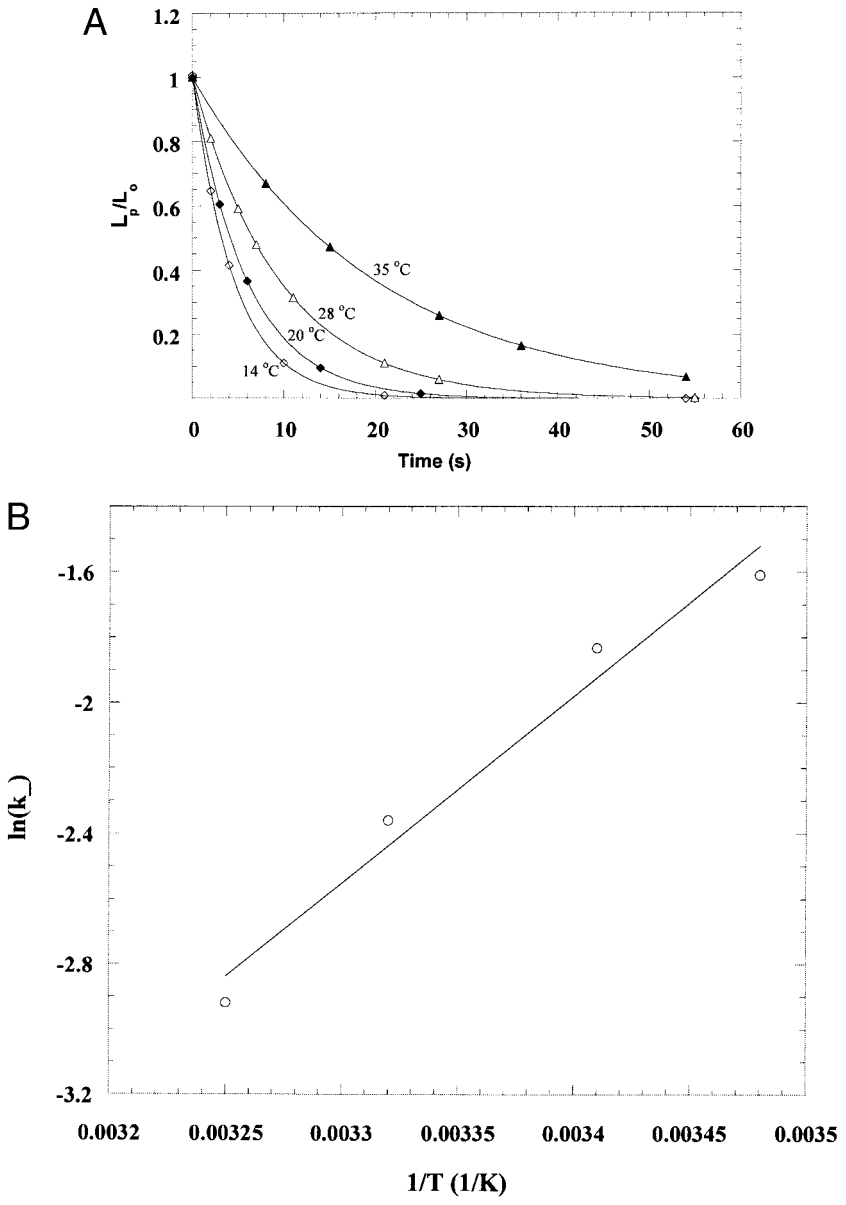

FIGURE 8 (*A*) Kinetics of peptide desorption at different temperature characterized by the change of the vesicle projection length measured with the micropipette assay during peptide washing. (*B*) Logarithm of the rate of peptide desorption verses the inverse temperature. The measurements were performed at pH 5.5.

phan blue shift, and Ac4K helicity) changed continuously with the decrease of the pH down to pH 4.5.

Effect of AcE4K binding on the properties of SOPC membranes

The intercalation of AcE4K in the membrane clearly changed membrane composition. This change of membrane composition could result in change of the membrane properties, such as the strength of the membrane, its permeability for water, and its area expansion modulus. The strength of the membrane was characterized by the tension for membrane failure (critical membrane tensions). For SOPC vesicles in glucose, the critical membrane tension was 10.5 ± 1 mN/m. The critical membrane tension in peptide-free buffer at pH 5 was 9.5 ± 1 mN/m, and, for buffer containing 10 μM peptide, at pH 5 it was 5.8 ± 1.1 mN/m. The critical membrane tension was measured also immediately after peptide desorption and it was 5.3 ± 2 mN/m. These measurements showed that the presence of the intercalated peptide decreased the membrane strength. However, this decrease was similar to the decrease of the membrane strength when the vesicles were transferred from glucose solution to peptide-free buffer. The similarity of the membrane strength after peptide desorption to the membrane strength in the presence of peptide suggested that, immediately after desorption, there were still traces of peptide present in the membrane.

The resistance of the membrane for area dilation was characterized by the area expansion modulus (Kwok and

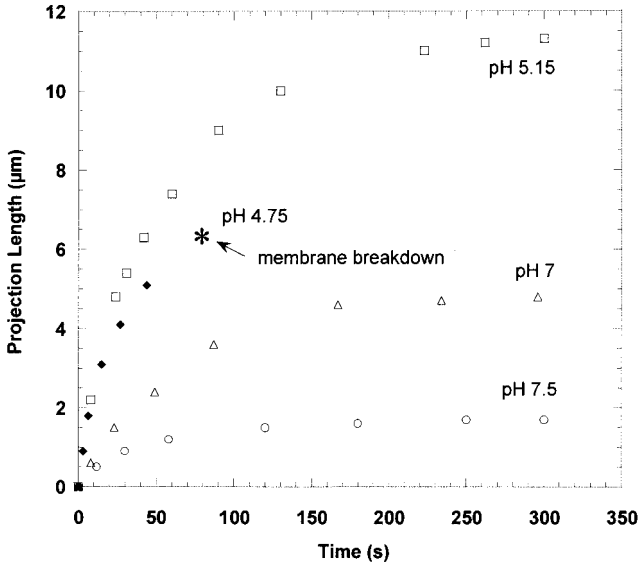

FIGURE 9 The exposure of single giant SOPC vesicles to peptide solutions resulted in an increase of the vesicle projection length inside the holding pipette. The magnitude of the projection length increase was dependent on pH and increased with the decrease of the pH. For pH 4.75, the vesicle broke down during adsorption. The peptide concentration was 10 μM.

Evans 1981; Needham and Nunn, 1990; Needham and Zhelev, 1996). The area expansion modulus could not be measured in the presence of inserted peptide because the volume of the vesicles changed continuously. The continuous change of the vesicle volume made it impossible to distinguish between the change of the vesicle projection length due to the volume change and due to the applied tension. The area expansion modulus was measured for the same vesicle before and after desorption (not shown). This measurement showed that the area expansion modulus after peptide desorption was equal to the area expansion modulus before peptide adsorption. This finding confirmed the conclusion made earlier that AcE4K desorbs almost completely after the transfer of the vesicles in peptide-free buffer.

We measured the permeability of the membrane for water both in the absence and presence of inserted peptide. The permeability of the membrane for water was sensitive to the ordering of the membrane lipids close to the membrane interface (Olbricht et al., 2000). This sensitivity was attributed to the presence of free volume in the hydrocarbon region close to the membrane interface (Marrink and Brensen, 1994; Marrink and Berkowitz, 1995). The measurement of the permeability for water of SOPC membranes with and without adsorbed peptide showed that the membrane permeability for water was independent of the presence of intercalated peptide (not shown). This result suggested that the insertion of AcE4K in the membrane did not perturb significantly the packing of the hydrocarbon region close to the membrane interface. This was another confirmation to the conclusion from the parallax measurements that AcE4K did not insert deep into the hydrocarbon region.

Effect of peptide insertion on membrane stability below pH 4.8

The breakdown of the vesicle membrane in the coarse of peptide adsorption for pH below 4.8 (Fig. 9) showed that either the membrane stability was compromised or the adsorbing peptide acquired a capability to disturb significantly the structure of the membrane. The measurement of membrane strength for the range of pH from 5.5 to 4.5 showed that the strength of the membrane was not affected by the decrease of pH (not shown). Therefore, the reduced membrane stability below pH 4.8 was attributed to the insertion of the peptide in the membrane. The threshold pH for membrane instability was very close to the measured pH on the order of 4.6 for the aggregation of AcE4K in concentrated peptide solutions. Also, the threshold pH was close to the pK of 4.7 for the three glutamatic acids and the aspartic acid of AcE4K. Therefore, there was a possibility that membrane breakdown was a result of membrane defects initiated by peptide aggregates. If such aggregates were present, their concentration was small compared to the concentration of the single peptide molecules, because below pH 4.8 we did not observe either tryptophan blue shift or the formation of α-helical structures in the absence of lipid. Two possibilities were considered: aggregate formation by the already adsorbed peptide, and aggregate formation in the solution before adsorption and fusion of peptide aggregates with the membrane. To distinguish between these two possibilities, we tried to protect the vesicle membrane against adsorption of peptide aggregates by using grafted poly(ethylene glycol) (PEG). We had shown (Needham et al., 1997) that the grafted PEG reduced the rate of micelle fusion with the membrane during the exchange of lysolipid with SOPC membranes. We wanted to use grafted PEG to prevent the peptide aggregates from reaching the membrane surface and inducing membrane breakdown. However, the use of grafted PEG at concentrations that almost completely inhibited micelle fusion (Needham et al., 1997) were not sufficient to reduce the destabilizing effect of the adsorbing AcE4K. (The vesicles with grafted PEG broke similarly to the vesicles without grafted PEG.) This lack of protection by the grafted PEG was either due to polymer precipitation at low pH or loss of protection due to the different nature of the interaction of the grafter polymer and the peptide aggregates, compared to the grafted PEG–micelle interactions.

Another possibility for the lack of protection by the grafted PEG was the possible aggregation of the already adsorbed peptide in the membrane. We tested this possibility by initially adsorbing AcE4K to the membrane at pH 5.5, and then exposing the membrane with the adsorbed peptide to peptide-free buffer at pH 4.7. The result from this test

was that the peptide desorbed, similar to the peptide desorption at pH 5.5. Thus, either the rate of peptide desorption was faster than the rate of aggregation, or the aggregation of the peptide in the membrane was not the factor determining membrane instability. We continued to explore these possibilities by initially adsorbing peptide at pH 5.4 and then transferring the vesicle with the adsorbed peptide to a solution with pH 4.7, which contained the same amount of peptide as the initial solution (Fig. 10). In these experiments, we measured the change of the vesicle projection length in the holding pipette and the lifetime of the vesicle after exposure to the peptide solution at pH 4.7. The measurements were compared to the same measurements when a single vesicle was exposed directly to peptide solution at pH 4.7 (Fig. 10). The experimental data showed that the presence of already adsorbed peptide increased the lifetime of the vesicles in the peptide solution with pH 4.7. The membrane lifetime in the presence of pre-adsorbed peptide was 220.2 ± 26.9 s, and that for direct exposure to peptide solution with pH 4.7 was 85.8 ± 7.6 s. Another important difference between the two sets of measurements was that the vesicles exposed directly to peptide solution at pH 4.7 broke instantaneously, whereas the vesicles with already adsorbed peptide swelled. The swelling of the vesicles suggested that there were stable and solute-selective pores with average size on the order of 5 nm, which were able to transport selectively glucose and small ions from the surrounding buffer, but not sucrose, from the vesicle interior. As a result, the sucrose-loaded vesicles swelled until breaking down (Fig. 10). These measurements showed that membrane instability was not caused by the aggregation of the adsorbed peptide molecules in the membrane, but rather was initiated by species formed in the bulk. We speculate that these species are peptide aggregates formed in the solution, because peptide monomers exchanged with the membrane at pH 4.7 in a similar way as they did at pH 5.5.

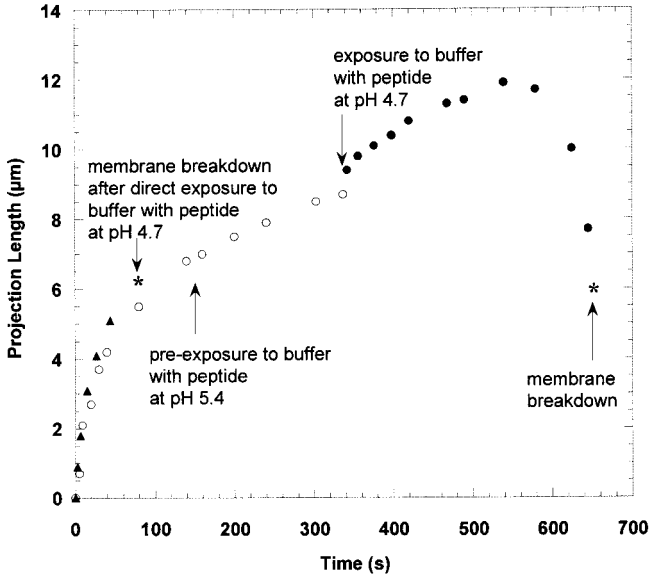

FIGURE 10 Change of the vesicle projection length after direct exposure to peptide solution with pH 4.7 (*triangles*), initial exposure to peptide solution with pH 5.5 (*open circles*), and then exposure to peptide solution with pH 4.7 (*closed circles*). The direct exposure of the vesicle to peptide solution at pH 4.7 resulted in vesicle breakdown during adsorption. The exposure of the vesicle to peptide solution with pH 5.5 led to increase of the projection length. The subsequent exposure to peptide solution at pH 4.7 resulted in additional increase of the projection length and then fast decrease of the projection length. The increase of the projection length could be a result of additional area change or volume loss. The fast decrease of the projection length was a result of pore formation and vesicle swelling. The peptide concentration was 10 μM.

The final set of measurements was designed to test the reversibility of the peptide-induced pore formation. In these measurements, stable selective pores were formed in the membrane of a single vesicle. The pores caused the vesicle to swell. In the course of swelling, the vesicle was exposed to peptide-free solution with the same pH (Fig. 11). Almost immediately after the exposure of the vesicle to the peptide-free solution the swelling stopped and the adsorbed peptide started to desorb. This result showed that the binding of the peptide in the pore region was reversible.

DISCUSSION

The binding of the AcE4K peptide to SOPC membranes studied in this work was coupled with an increase of the membrane area. The increase of membrane area showed that AcE4K was inserted in the membrane interior. This behavior was consistent with the increase of the surface pressure of lipid monolayers upon the binding of the similar peptide E4 (Rafalski et al., 1991). Similar coupling between peptide binding and membrane area increase was measured also for the wild-type w-20 peptide from the X31 influenza virus (Longo et al., 1997, 1998). The binding of E4 to the membrane was similar to the binding of w-20 and the primary amino sequence of the two peptides was identical except for one amino acid (E4 had at fourth position a glutamatic acid, whereas w-20 had a glycine, Rafalski et al. 1991). AcE4K was similar to E4, except that its N terminal was acetylated and it had lysine at its C terminal. Therefore, the binding of AcE4K to the SOPC membrane was compared to the similar binding of E4 and w-20. The importance of the N terminal for the binding of HA2 was demonstrated by Gething et al. (1986) and others (Burger et al., 1991; Steinhauer et al., 1995; Gray et al., 1996). They showed that the removal of the glycine at the N terminal completely abolishes the binding of w-20 to the membrane and the formation of α-helical structures by the peptide. In contrast, the acylation of the N terminal enhanced the formation of α-helical structures in nonpolar solvents (Rohl et al., 1996). Therefore, the acylation of the N terminal of AcE4K was not expected to affect adversely its ability to bind to the SOPC membrane. The presence of the lysine at the C-terminal of AcE4K increased the overall positive charge of the peptide.

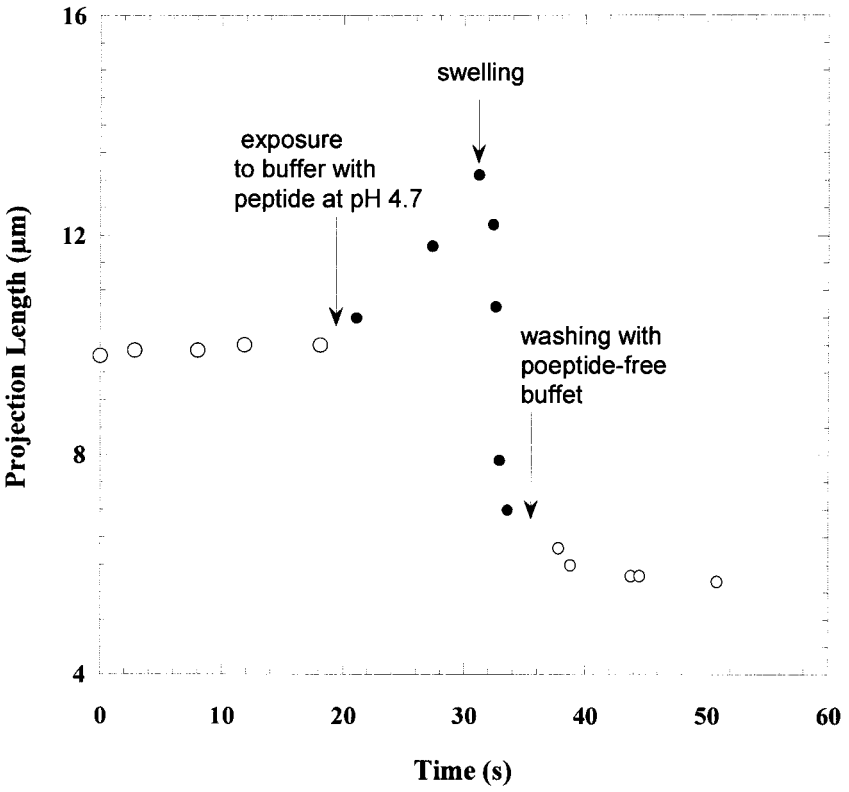

FIGURE 11 Reversible pores stimulated by AcE4K. The formation of pores was stimulated by exposing a single vesicle to peptide solution with reduced peptide concentration and with pH 4.7. After pore formation, the vesicle started to swell, and its projection length in the holding pipette started to decrease. During swelling, the vesicle was exposed to peptide free buffer with pH 4.7. The exposure to the peptide free buffer arrested the swelling of the vesicle and its projection length in the holding pipette approached a steady state. (The slow decrease of the projection length after the beginning of washing was due to peptide desorption.

However, this was not expected to affect significantly the binding of the peptide, because EPR measurement of the position of w-20 in the membrane (Zhou et al., 2000) suggested that the side chain of the lysine at the C terminal would partition in the lipid headgroup region of the membrane. The parallax measurements showed that the tryptophan side chain of AcE4K inserted to the same depth as the same side chain of w-20, confirming that the presence of the lysine at the C terminal did not affect adversely the insertion of the peptide.

The insertion of AcE4K in the membrane increased the membrane area. In a microscopic scale, this peptide insertion required rearrangement of the lipid molecules in one of the membrane monolayers and the formation of a vacancy for the peptide. The overall free energy change accompanying this process had two major components, one related to the change of the free energy of the peptide during its transition from the water solution to the membrane interface, and the other related to the change of the free energy of the membrane. We consider the work for creating a vacancy to be related to the change of the free energy of the membrane.

Due to the difference of the accessibility of the inside and the outside membrane monolayers, the inserted peptide initially partitions in the outside membrane monolayer. The asymmetry of the initial peptide distribution between the two membrane monolayers creates intermonolayer stress, which is coupled with change of the membrane free energy. This stress is eventually relaxed as either peptide molecules or lipids or both are transferred across the membrane. Another source of change of the membrane free energy arises from the difference of the packing conditions of the lipids bordering the inserted peptide molecules, and the lipids away from the sites of insertion. The change of lipid packing is characterized using mean-field membrane elasticity (Dan and Safran, 1995; Nielsen et al., 1998). In this case, the change of the membrane free energy is independent of time and represents the equilibrium change of the membrane free energy due to molecular insertion. The equilibrium free energy has been modeled extensively (May, 2000) because of its importance for channel activity (Lundbaek et al., 1997; Lundbaek and Andersen, 1999; Lewis and Cafiso, 1999).

The exchange of AcE4K with SOPC vesicles held by micropipettes presented in this work is characterized by both the equilibrium and the nonequilibrium change of the membrane free energy. The modeling of the equilibrium change of the membrane free energy is done successfully for symmetrical vacancies, such as the inclusion vacancy for the gramicidin channel (May, 2000). The overall predictions of the models is that the magnitude of the increase of the free energy depends almost linearly on the mismatch between the membrane thickness and the apparent hydrophobic thickness of the inserted molecule (Lundbaek and Anderson, 1999). The exact geometry of the vacancy of AcE4K (or the wild-type wt-20 peptide) is unknown. How-

ever, this geometry is expected to be complex due to the almost perpendicular orientation of the peptide relative to the membrane normal (Zhou et al., 2000). The insertion of the similar helical peptide maganin 2 in phophatidylcholine membranes (Ludtke et al., 1995) showed that peptide insertion was coupled with decreasing the membrane thinning. Then, if the membrane thickness decreases with the insertion of AcE4K, the mismatch at the boundary of the inserted peptide will be similar to the initial stage of pore formation. Then, if the mismatch is significant, we expect to observe a significant decrease of the membrane tensile strength in the presence of inserted peptide. The measurement of the membrane tensile strength in the presence and the absence of AcE4K (see *Effect of AcE4K binding on the properties of SOPC membranes* in the Results section), showed that there was no significant decrease of the membrane strength in the presence of peptide. Similar results were obtained for the wild-type wt-20 peptide by Longo et al. (1998). In the same paper, the authors showed that the modification of wt-20 by attaching fluorescein to its N terminus resulted in making a modified peptide, which both substantially decreased the membrane strength and compromised the ability of the membrane to retain solutes. These data taken together suggest that the insertion of AcE4K in the SOPC membrane does not significantly change the equilibrium free energy of the membrane.

The exchange of the AcE4K with the membrane results in change of the number of molecules in the membrane. For example, the insertion of each peptide molecule in the membrane requires the creation of a vacancy for the peptide molecule to fit between the membrane lipids. The creation of the vacancy requires work and is coupled with a compression of the outside membrane monolayer and an extension of the inside membrane monolayer. The stress between the two membrane monolayers will be eventually relaxed. However, the time of relaxation could be much longer than the time of peptide insertion. Therefore, the work for creating a vacancy can be considered a temporary loss of free energy of binding for the inserted molecule and should be considered when measuring the rate of peptide adsorption and desorption. The exchange of AcE4K with the membrane occurs within several minutes (Figs. 6, 8 *A*, and 9). This corresponds to desorption rates on the order of 0.13 s^{-1}, which is similar to the rate of desorption of the lysolipid MOPC from SOPC membranes (Needham and Zhelev, 1995). Because AcE4K does not form large pores in the membrane, one can anticipate rates of forced lipid transfer across the membrane (or forced flip flop, Fattal et al., 1994), on the order of 0.003 s^{-1} (Needham and Zhelev, 1995). Thus, both the adsorption of the peptide to the membrane and its desorption will involve predominantly the peptide inserted in the outside membrane monolayer. The work of creating a vacancy in the outside membrane monolayer during peptide adsorption is calculated from the product of the monolayer tension and the area of the vacancy. These two characteristics could be determined from the micropipette measurements of the area expansion modulus of the membrane in absence of peptide and the measured vesicle area changes during peptide desorption.

In the experiments of peptide desorption, the vesicle was incubated in the peptide solution for about 10 min and then the adsorbed peptide was desorbed by flowing peptide-free solution over the vesicle (Fig. 6). The characteristic time of desorption was on the order of 5 min, however the half time of desorption was on the order of 5 to 15 s (Fig. 8 *A*). In these conditions, the peptide partitioned mainly in the outside vesicle monolayer. Then the work for the insertion of one mole of peptide W_v^0 was calculated by (Zhelev, 1998)

$$W_v^0 = K \frac{A_p^2}{A_{lp}} N_a, \tag{9}$$

where K was the area expansion modulus, A_p was the area occupied by a single peptide molecule, A_{lp} was the initial area occupied by the lipids associated with the inserted peptide, and N_a was the Avogadro number.

The area A_{lp} was found from the peptide concentration in the membrane C_{pm} (on molar ratio basis), when 10 μM peptide was present in the solution. The peptide concentration C_{pm}, corresponding to the partition coefficient K_p, was calculated from $C_{pm} = K_p C_{ps}$, where C_{ps} was the bulk peptide concentration. The partition coefficient for pH 5.5 was 4.8×10^4, then the calculated peptide concentration in the membrane was $C_{pm} = 8.63 \times 10^{-3}$. The number of lipid molecules per one bound peptide at pH 5.5 was 116. The lipid molecules associated with a single peptide molecule were present in the two membrane monolayers, then the number of associated lipid molecules in one of the membrane monolayers was 58. The area of a single SOPC molecule was on the order of 65 $Å^2$ (McIntosh and Simon, 1986). Then 58 lipids had an area of 3770 $Å^2$. The measured 6% vesicle area change during peptide desorption corresponded to an area per peptide molecule A_p on the order of 226 $Å^2$. This value for the area per peptide molecule was similar to the area of 120 $Å^2$ or more occupied by the mutant E4 in phosphatidylcholine monalyers at surface pressure equal to the apparent bilayer pressure (Rafalski et al, 1991). Ishiguro et al. (1996), considered the volume occupied by the wild-type HA2 peptide, assuming that the peptide was almost parallel to the membrane interface, and estimated its area to be on the order of 300 $Å^2$. This area was also similar to the measured area of AcE4K. The area expansion modulus K of the SOPC membrane, was chosen equal to 190 (mN/m) (Needham and Nunn, 1990; Zhelev, 1998). Then the work for insertion of one mole of peptide in the membrane was 15.5 kJ/mol (3.7 kcal/mol).

The mean field approximation used here allowed an estimate of the apparent interfacial tension of the bound peptide. The contact area between the peptide and the membrane had an apparent interfacial tension. This apparent

interfacial tension of the peptide contact area was calculated from the ratio of the Gibbs energy for peptide transfer to the area occupied by the inserted peptide. The calculated apparent interfacial tension was on the order of 20 mN/m. This value was somewhat smaller than the value of the apparent interfacial tension for the membrane hydrocarbon region on the order of 33 mM/m (Zhelev, 1998). The calculation of the latter apparent interfacial tension was based on the measured activation energy for transfer of a single hydrocarbon to water, which was on the order of 0.68 kcal/mol (Israelashvili, 1991). Another interfacial tension for comparison would be the alkane–water interfacial tension, equal to 50 mN/m (Small, 1986), which represented the maximum possible hydrocarbon–water interfacial tension. The comparison of the above interfacial tensions suggests that the gain in free energy due to the removal of the hydrophobic amino acid side chains from their water environment is a major driving force for the binding of AcE4K to the membrane.

The dominant role of the hydrophobic interactions for the binding of AcE4K was also suggested by the correlation between peptide binding and amino acid protonation. The presented experimental data showed that the partitioning of AcE4K increased with the decrease of the solution's pH. The partitioning was minimum for pH 7 and maximum for pH 4.5. The measured partition coefficients were 3.1×10^2 for pH 7 and 3.2×10^6 for pH 4.5 (Fig. 4 *A*). The corresponding Gibbs energies were 14.1 kJ/mol (3.4 kcal/mol) and 37.1 kJ/mol (8.9 kcal/mol), respectively. Thus, the apparent change of the Gibbs energy due to the protonation of AcE4K from pH 7 to 4.5, was 23 kJ/mol (5.5 kcal/mol). The amino acids expected to be protonated were the three glutamatic acids and the aspartic acid, with pK of 4.7. The Gibbs energies for transfer of these amino acids from water to the phosphatidylcholine membrane were measured by Wimley and White (1996) and were −2.02 kcal/mol for Glu and −1.23 kcal/mol for Asp at pH 8, and 0.01 kcal/mol for Glu and 0.07 kcal/mol for Asp at pH 2. Thus, there was a difference of −7.4 kcal/mol of the change of the Gibbs energy, when the three glutamatic acids and the aspartic acid were transferred to the membrane at pH 8 and pH 2, respectively. This change of the Gibbs energy was very close to measured change of the Gibbs energy on the order of −5.5 kcal/mol for the binding of AcE4K at pH 7.5 and 4.5, respectively. The similarity of the change of the two Gibbs energies suggested that the binding of AcE4K to the SOPC membrane was directly related to the protonation of the glutamatic acids and the acpartic acid.

The observation that the depth of insertion of AcE4K in the membrane was independent of pH was consistent with the similar finding for the wild-type HA2 fusion peptide (Luneberg et al., 1995; Zhou et al., 2000). The independence of the depth of insertion on pH suggested that the membrane provided an interface for the folding of the peptide, while the amount of adsorbed peptide at steady state was dependent on the peptide's bulk concentration and the pH. In this regard, it was instructional to compare the blue shift of the tryptophan fluorescence and the CD spectra of the soluble AcE4K measured in this work and the same characteristics for the Lipo-AcE4K (Bailey et al. 1997). The maximum tryptophan fluorescence of the soluble AcE4K at pH 7.5 was measured at 355 nm, whereas the maximum fluorescence for Lipo-AcE4K at the same pH was measured at 340 nm (Bailey et al. 1997). This apparent blue shift of the maximum fluorescence for the lipid-linked peptide relative to the fluorescence for the soluble peptide suggested that the lipid-linked peptide was in more hydrophobic environment compared to the soluble peptide. Compared to pH 7.5, the maximum tryptophan fluorescence for pH 5 had a blue shift of 14 nm (Fig. 1), whereas that for the Lipo-AcE4K had a blue shift of 12 nm. These results showed that the blue shift of both peptides was similar. However, the lipid-linked peptide was partially inserted in the membrane at neutral pH. In contrast, the dependence of peptide helicity on pH was different for the two peptides. The helicity of the soluble peptide was dependent on pH. For pH 7.5, there were almost no α-helical structures, but for pH 5 almost half of the peptide was in α-helical conformation (Fig. 2 *B*). In contrast, the conformation of the lipid-linked peptide was always α-helical and independent of pH (Bailey et al., 1997). The measured CD spectra for the Lipo-AcE4K (Bailey et al., 1997) resembled with high accuracy the CD spectra measured at pH 4.5 for the soluble peptide (Fig. 2 *A*). This comparison of the two peptides showed that the lipid-anchored peptide was folded in its own membrane. The additional blue shift at low pH of the Lipo-AcE4K and its ability to assist the trafficking of lipid between membranes (Bailey et al., 1997), suggested that, for low pH, the Gibbs energy of binding to the opposing membrane was lower than the energy of binding to the same membrane. The conclusion that the increase of the measured helicity of the soluble peptide was a result of an increase of the number of inserted molecules while the depth of insertion was the same, and the finding that the CD spectra of the Lipo-AcE4K resemble the spectra for maximum binding of AcE4K, suggested that the peptide from the lipo-peptide was always inserted in the membrane. Thus, the linkage of the peptide to the lipid lowered the energy of peptide insertion in the membrane.

The insertion of the peptide in the membrane also affected the membrane mechanical properties. The ability of the inserted peptide to disturb the membrane structure and compromise the membrane stability was dependent on pH. Below the threshold pH of 4.8, the inserted peptide created membrane pores, which led to membrane breakdown. The pores formed by the adsorbed peptide were reversible, which showed that the binding of the peptide in the pore region was reversible. The formation of membrane pores alone did not lead to membrane fusion. We performed a test for membrane fusion by holding two in contact while ex-

posing them to peptide solution at pH 4.7. In all measurements, the membranes broke down and no fusion events were observed. The absence of fusion events suggested that the species promoting defect formation were inserted into the membrane and could not provide the necessary bridging between the membranes in the contact region. This was consistent with the similar finding for the other HA2 fusion peptide mutants, which also were not able to fuse large unilamellar vesicles (Wilshut and Bron, 1993).

CONCLUSION

In conclusion, we showed that the HA2 fusion peptide mutant AcE4K inserts in the membrane of SOPC vesicles in a pH-dependent manner. For pH above 5, this insertion did not significantly affect the stability (tensile strength or pore formation) of the membrane, but below pH 4.85, the stability of the membrane was significantly compromised. The inserted peptide resigned close to the membrane interface, which was demonstrated by fluorescence quenching. The inserted peptide occupied an area in the membrane on the order of 200 $Å^2$ per peptide molecule. This area led to a significant increase of the total membrane area after peptide adsorption. The adsorption of the peptide was characterized by the change of the Gibbs energy of binding. The Gibbs energy of binding increased with the decrease of the pH and was maximum for pH 4.5. With the decrease of the pH, the number of the bound molecules increased, but the depth of insertion of the individual molecules in the membrane was independent of pH. This finding allowed us to use a simple model for the binding of AcE4K, where the binding of each peptide was coupled with doing work for creating a vacancy for the peptide molecule in the membrane. The calculation of this work for creating a vacancy for pH 5.5 showed that the work for creating a vacancy was an important determinant of the rate of peptide binding. Our data suggested that the binding of the peptide to the membrane was driven by hydrophobic interactions. The pH dependence of the peptide binding was due to peptide protonation and an apparent increase of the peptide hydrophobicity.

This work was supported by grants GM 40162 and HL57629 from the National Institutes of Health.

REFERENCES

Alford, D., H. Ellens, and J. Bentz. 1994. Fusion of influenza virus with sialic acid-bearing target membranes. *Biochemistry.* 33:1977–1987.

Bailey, A. L., M. A. Monk, and P. R. Cullis. 1997. pH-induced destabilization of lipid bilayers by a lipopetide derived from influenza hemagglutinin. *Biochim. Biophys. Acta.* 1324:232–244.

Bentz, J. 2000. Membrane fusion mediated by coiled coils: a hypothesis. *Biophys. J.* 78:886–900.

Bentz, J., H. Ellens, and D. Alford. 1990. An architecture for the fusion site of influenza hemagglutinin. *FEBS Lett.* 276:1–5.

Bullough, P. A., F. M. Hughson, J. J. Skehel, and D. C. Wiley. 1994. Structure of influenza haemagglutinin at the pH of membrane fusion. *Nature.* 371:37–43.

Burger, K. N. J., S. A. Wharton, R. A. Demel, and A. J. Verkleij. 1991. The interaction of synthetic analogs of the N-terminal fusion sequence of influenza virus with a lipid monolayer. Comparison of fusion-active and fusion defective analogs. *Biochim. Biophys. Acta.* 1065:121–129.

Chang C. T., C.-S. C. Wu, and J. T. Yang. 1978. Circular dichroic analysis of protein conformation: inclusion of the β-turns. *Anal. Biochem.* 91: 13–31.

Chattopadhyay, A., and E. London. 1987. Parallax method for direct measurement of membrane penetration depth utilizing fluorescence quenching by spin-labeled phospholipids. *Biochemistry.* 26:39–45.

Chernomordic, L., V. A. Frolov, E. Leikina, P. Bronk, and J. Zimmerberg. 1998. The pathway of membrane fusion catalyzed by influenza hemagglutinin: restriction of lipids, hemifusion, and lipidic fusion pore formation. *J. Cell Biol.* 140:1369–1382.

Dan, N., and S. A. Safran. 1995. Solubilization of proteins in membranes. *Israel J. Chem.* 35:37–40.

Danieli, T., S. L. Pelletier, Y. I. Henis, and J. M. White. 1996. Membrane fusion mediated by the influenza virus hemagglutinin requires the concerted action of at least three hemagglutinin trimers. *J. Cell Biol.* 133:559–569.

Durrer, P., C. Galli, S. Hoenke, C. Corti, R. Gluck, T. Vorherr, and J. Brunner. 1996. H^+-induced membrane insertion of influenza virus hemagglutinin involves the HA2 amino-terminal fusion peptide but not the coiled coil region. *J. Biol. Chem.* 271:13417–13421.

Evans, E. A., and Skalak, R. 1980. Mechanics and Thermodynamics of Biomembranes. CRC Press, Boca Raton, FL.

Fattal, E., S. Nir, R. A. Parente, and F. C. Szoka. 1994. Pore-forming peptides induce rapid phospholipid flip-flop in membranes. *Biochemistry.* 33:6721–6731.

Gaudin, Y., R. W. Ruigrok, and J. Brunner. 1995. Low-pH induced conformational changes in viral fusion proteins: implications for the fusion mechanism. *J. Gen. Virol.* 76:1541–1556.

Gething, M.-J., R. W. Doms, D. York, and J. M. White. 1986. Studies on the mechanism of membrane fusion: site-specific mutagenesis of the hemagglutinin of the influenza virus. *J. Cell Biol.* 107:11–23.

Gray, C., S. A. Tatulian, S. A. Wharton, and L. K. Tamm. 1996. Effect of N-terminal glycine on the secondary structure, orientation, and interaction of the influenza hemagglutinin fusion peptide with lipid bilayers. *Biophys. J.* 70:2275–2286.

Harter, C., P. James, T. Bachi, G. Semenza, and J. Brunner. 1989. Hydrophobic binding of the ectodomain of influenza hemagglutinin to membranes occurs through the "fusion peptide." *J. Biol. Chem.* 264: 6459–6464.

Ishiguro, R. N., M. Matsumoto, and S. Takahashi. 1996. Interaction of fusogenic synthetic peptide with phspholipid bilayers: orientation of the peptide α-helix and binding isotherm. *Biochemistry.* 35:4976–4983.

Israelashvili, J. N. 1991. Intermolecular and Surface Forces. Academic Press, San Diego, CA. 354.

Kemble, G. W., T. Danieli, and J. M. White. 1994. Lipid-anchored influenza hemagglutinin promotes hemifusion, not complete fusion. *Cell.* 76:383–391.

Kwok, R., and E. A. Evans. 1981. Thermoelasticity of large lecithin bilayer vesicles. *Biophys. J.* 35:637–652.

Lakowicz, J. R., and S. Keating. 1983. Binding of an indole derivative to micelles as quantified by phase-sensitive detection of fluorescence. *J. Biol. Chem.* 258:5519–5524.

Lear, J. D., and W. F. DeGrado. 1987. Membrane binding and conformational properties of peptides representing the NH_2 terminus of influenza HA2. *J. Biol. Chem.* 262:6500–6504.

Lewis, J. R., and D. S. Cafiso. 1999. Correlation between the free energy of a channel-forming voltage-gated peptide and the spontaneous curvature of bilayer lipids. *Biochemistry.* 38:5932–5938.

Longo, M. L., A. J. Waring, and D. A. Hammer. 1997. Interaction of the hemagglutinin fusion peptide with lipid bilayers: area expansion and permeation. *Biophys. J.* 73:1430–1439.

Longo, M. L., A. J. Waring, L. M. Gordon, and D. A. Hammer. 1998. Area expansion and permeation of phospholipid membrane bilayers by influenza fusion peptides and mellitin. *Langmuir.* 14:2385–2395.

Lundbaek, J. A., A. M. Maer, and O. S. Andersen. 1997. Lipid bilayer electrostatic energy, curvature stress, and assembly of gramicidin channels. *Biochemistry.* 36:5695–5701.

Lundbaek, J. A., and O. S. Andersen. 1999. Spring constants for channel-induced lipid bilayer deformations. Estimates using gramicidin channels. *Biophys. J.* 76:889–895.

Ludtke, S., K. He, and H. Huang. 1995. Membrane thinning caused by maganin 2. *Biochemistry.* 34:16764–16769.

Luneberg J., I. Martin, F. Nussler, J. M. Ruysschaert, and A. Herrmann. 1995. Structure and topology of the influenza virus fusion peptide in lipid bilayers. *J. Biol. Chem.* 270:27606–27614.

Macosko, J. C., C.-H. Kim, and Y.-S. Shin. 1997. The membrane topology of the fusion peptide region of influenza hemagglutinin determined by spin-labeling EPR. *J. Mol. Biol.* 267:1139–1148.

Marrink, S. J., and H. L. C. Brendsen. 1994. Simulation of water transport through a lipid membrane. *J. Phys. Chem.* 98:4155–4168.

Marrink, S. J., and M. Berkowitz. 1995. Water and membranes. *In* Permeability and Stability of Lipid Bilayers. E. A. Disalvo and S. A. Simon, editor. CRC Press, Boca Raton, FL. 19–46.

Martin, K., H. Reggio, A. Helenius, and K. Simons. 1981. Infectious entry pathway of influenza virus in a canine kidney cell line. *J. Cell Biol.* 91:601–613.

May, S. 2000. Theories on structural perturbations of lipid bilayers. *Curr. Opin. Colloid Interface Sci.* 5:244–249.

McIntosh, T. J., and S. A. Simon. 1986. Hydration force and bilayer deformation: a reevaluation. *Biochemistry.* 25:4058–4066.

Melikyan, G. B., J. M. White, and F. S. Cohen. 1995. GPI-anchored influenza hemagglutinin induces hemifusion to both red blood cell and planar bilayer membranes. *J. Cell Biol.* 131:679–691.

Needham, D., and R. S. Nunn. 1990. Elastic deformation and failure of lipid membranes containing cholesterol. *Biophys. J.* 58:997–1009.

Needham, D., N. G. Stoycheva, and D. V. Zhelev. 1997. Exchange of monooleoylphosphatidylcholine as monomer and micelle with membranes containing polyethileneglycol-lipid. *Biophys. J.* 73:2615–2629.

Needham, D., and D. V. Zhelev. 1995. Lysolipid exchange with lipid vesicle membranes. *Annals Biomed. Eng.* 23:287–298.

Needham, D., and D. V. Zhelev. 1996. Mechanochemistry of lipid vesicles examined by micropipet manipulation. *In* Vesicles. M. Rosoff, editor. Marcel Dekker, New York and Basel. 373–444.

Nielsen, C., M. Goulian, and O. S. Andersen. 1998. Energetics of inclusion-induced bilayer deformations. *Biophys. J.* 74:1966–1983.

Olbrich K. C., W. Rawicz, D. Needham, and E. Evans. 2000. Water permeability and mechanical strength of polyunsaturated phospholipid bilayers. *Biophys. J.* 79:321–327.

Rafalski, M., A. Ortiz, A. Rockwell, L. C. van Ginkel, J. D. Lear, W. F. DeGrado, and J. Wilshut. 1991. Membrane fusion activity of the influenza virus hemagglutinin: interaction of HA2 N-terminal peptides with phospholipid vesicles. *Biochemistry.* 30:10211–10220.

Rogers, G. N., J. C. Paulson, R. S. Daniels, J. J. Skehel, I. A. Wilson, and D. C. Wiley. 1983. *Nature.* 304:76–78.

Rohl, C. A., A. Chakrabartty, and R. L. Baldwin. 1996. Helix propagation and N-cap propensities of the amino acids measured in alanine-based peptides in 40 volume percent trifluoroethanol. *Protein Sci.* 5:2623–2637.

Ruigrok, R. W. H., A. Aitken, L. J. Calder, S. R. Martin, J. J. Skehel, S. A. Wharton, W. Weis, and D. C. Wiley. 1988. Studies on the structure of the influenza virus hemagglutinin at the pH of membrane fusion. *J. Gen. Virol.* 69:2785–2795.

Sauter, N. K., M. D. Bernarski, B. A. Wutzburg, J. E. Hanson, G. M. Whitesides, J. J. Skehel, D. C. Wiley. 1989. Hemagglutinin from two influenza virus variants bind to sialic acid derivatives with millimolar dissociation constants: a 500-MHz proton nuclear magnetic resonance study. *Biochemistry.* 28:8388–8396.

Schroth-Diez, B., E. Ponimaskin, H. Reverey, M. F. Schmidt, and A. Herrmann. 1998. Fusion activity of transmembrane and cytoplasmic domain chimeras of the influenza virus glycoprotein hemagglutinin. *J. Virol.* 72:133–141.

Seelig, J. 1997. Titration calorimetry of lipid–peptide interactions. *Biochim. Biophys. Acta.* 1331:103–116.

Shangguan, T., D. Alford, and J. Bentz. 1996. Influenza virus-liposomes lipid mixing is leaky and largely insensitive to the material properties of the target membrane. *Biochemistry.* 35:4956–4965.

Small, D. M. 1986. Handbook of Lipid Research. Vol. 4. D. J. Hanahan, editor. Plenum Press, NY. 575.

Stegmann, T., and Helenius, A. 1993. Influenza virus fusion: from models toward a mechanism. *In* Viral Fusion Mechanisms. J. Bentz, editor. CRC Press, Boca Raton, FL. 89–111.

Stegmann, T., D. Hoekstra, G. Scherphof, and J. Wilshut. 1985. Kinetics of pH dependent fusion between influenza virus and liposomes. *Biochemistry.* 24:3107–3113.

Steinhauer D. A., S. A. Wharton, J. J. Skehel, and D. C. Wiley. 1995. Studies of the membrane fusion activities of fusion peptide mutants of influenza virus hemagglutinin. *J. Virol.* 69:6643–6651.

Takahashi, S. 1990. Conformation of membrane fusion-active 20-residue peptides with or without lipid bilayers. Implication of α-helix formation for membrane fusion. *Biochemistry.* 29:6257–6264.

Weber, T., G. Paesold, C. Galli, R. Mischler, G. Semenza, and J. Brunner. 1994. Evidence for H^+-induced insertion of influenza hemagglutinin HA2 N-terminal segment into viral membrane. *J. Biol. Chem.* 269: 18353–18358.

Wilshut, J., and R. Bron. 1993. The influenza virus hemagglutinin: membrane fusion activity in intact virions and reconstituted virosomes. *In* Viral Fusion Mechanisms. J. Bentz, editor. CRC Press, Boca Raton, FL. 133–161.

Wimley, W. C., and S. H. White. 1996. Experimentally determined hydrophobicity scale for proteins at membrane interfaces. *Nature Stuct. Biol.* 3:842–848.

Zhelev, D. V. 1996. Exchange of monooleoylphosphatidylchoiline with single egg phosphatidylcholine vesicle membranes. *Bophys. J.* 71: 257–273.

Zhelev, D. V. 1998. Material property characteristics for lipid bilayers containing lysolipid. *Biophys. J.* 110:1967–1977.

Zhou, Z., J. C. Macosko, D. W. Hughes, B. G. Sayer, J. Hawes, and R. M. Epand. 2000. ^{15}N NMR study of the ionization properties of the influenza virus fusion peptide in zwitterionic phospholipid dispersions. *Biophys. J.* 78:2418–2425.